

Title	Studies on Radiation Effects in CdTe Detectors
Author(s)	宮丸, 広幸
Citation	大阪大学, 1999, 博士論文
Version Type	VoR
URL	https://doi.org/10.11501/3155639
rights	
Note	

Osaka University Knowledge Archive : OUKA

<https://ir.library.osaka-u.ac.jp/>

Osaka University

Studies on Radiation Effects in CdTe Detectors

(CdTe 検出器の放射線効果に関する研究)

Hiroyuki Miyamaru

(宮 丸 広 幸)

1999

Abstract

In recent years, performance of CdTe detectors has been significantly improved by modern technology of crystal growth. This new detector has been becoming widely used in nuclear science, nuclear medicine, space science owing to its advantageous characteristics; room temperature operation, high detection efficiency, and low cost. When the field of application is widely grown, CdTe detectors may have an opportunity to be used in severe radiation environments such as nuclear domain and space. In an intense radiation environment, the detector is damaged by radiations and then its performance is markedly degraded. The evaluation of radiation hardness is thus important for performance stability and reliability of the detector. Although, some of basic radiation effects on CdTe itself are not well understood. A few experimental results related with gamma-ray irradiation have been reported for the CdTe detector, but the influence of fast neutrons and charged particles has never been investigated to date. Fast neutrons and charged particles are characterized by higher ability of defect creation and then they also affect the detector performance as well as high-energy photons. Progressive study for various radiations is now expected for further development of this new detector.

In this study, experiments to evaluate the performance of CdTe detectors after irradiation with fast neutrons and deuterium ions were undertaken in order to examine radiation effects. A pulse height spectrum of gamma rays from a standard radiation source was acquired from the irradiated detector. The radiation effect was evaluated from the change of the spectrum shape. In addition, electronic signal processing of rise time discrimination (RTD) was employed to obtain a two-dimensional (pulse amplitude-rise time) spectrum. The transport properties of both electrons and holes were also examined by analyzing the shape of a response pulse. On the fast neutron irradiation experiment, electron mobility and lifetime decreased with increasing the fast neutron fluence. In contrast, the hole transport property remained almost unchanged. The detector performance was found not to change significantly below the fluence of 1.0×10^{10} n/cm². Radiation hardness of the CdTe detector against 14 MeV fast neutrons was experimentally clarified. From the two-dimensional spectrum analysis, it

was suggested that a deep electron-trapping center was generated by fast neutrons in the CdTe crystal. In order to assign this center, isochronal annealing and thermally stimulated current (TSC) analysis were carried out for the irradiated CdTe. The experimental results supported that the characteristic of the electron-trapping center was quite similar to that of a Cd-related center.

Effects of deuterium (D) ion implantation were investigated for the CdTe detector. The electron mobility slightly increased for the detector implanted with lower fluence of D ions. This result indicated that the implanted D atoms played a role to passivate intrinsic defects of CdTe. On the other hand, the mobility markedly decreased in the higher fluence over 1×10^{14} ions/cm². Excess implantation was found to degrade the detector performance.

The pre-irradiation treatment with fast neutrons was conducted to the CdTe detector in order to improve radiation response characteristic for high-energy photons. Peak broadening of a photopeak was effectively suppressed by the pre-irradiation, and due to this, energy resolution of the pre-irradiated detector was successfully improved. When using the pre-irradiated detector with the RTD processing, further resolution enhancement was obtained. Application of the fast neutron irradiation effect to improve energy resolution of the CdTe detector was thus demonstrated.

要旨

近年の技術進歩によって目覚ましく性能が向上したテルル化カドミウム (CdTe)放射線検出器は、原子力関連分野はもとより核科学、核医療、宇宙科学等の幅広い分野で利用されるようになってきたが、その放射線に対する基本的影響が必ずしも良く理解されているわけではない。この検出器が常温で利用できる優れた X(γ)線検出器として今後様々な分野に応用されることを考えると、高線量の放射線が検出器の性能に対してどのような影響を与えるかを評価することは非常に重要である。現在までに γ 線による影響についてはわずかながら報告があるが、その影響が大きいと考えられる高速中性子や高エネルギー荷電粒子等については全く分かっていない。そこで本研究では CdTe 検出器に対するこれらの放射線の影響を調べることを目的として、高速中性子や、重水素イオンで照射された後の検出器の性能を評価する実験を行った。照射された検出器を用いて標準線源からの γ 線のエネルギースペクトルを測定し、その変化から照射の影響を評価した。また放射線の影響を詳細に調べる新しい手法としてパルス波高一立ち上がり時間の2次元スペクトル分析を用いた。更にパルス応答波形の解析から電子と正孔のキャリア輸送特性を調べた。

高速中性子の照射実験では、照射線量が増大するにつれて電子キャリアの移動度と寿命の減少が明確に観測された。これに対し正孔キャリアの輸送特性はほとんど変化が観測されなかった。また高速中性子照射実験においては、 1×10^{10} n/cm² 以下の線量では検出器性能に大きな変化はないことが分かった。この結果から CdTe 検出器の 14 MeV 高速中性子に対する耐性が実験的に明らかになった。また、2次元スペクトル分析の結果からは高速中性子照射によって CdTe 結晶中に深いエネルギー準位を持つ電子捕獲中心が生成されることが示唆された。この捕獲中心を同定するために、照射された CdTe 結晶に対して等時焼鈍実験と TSC (熱刺激電流) 分析を行った。実験結果から、この捕獲中心の性質がカドミウム原子やその空孔に関連した欠陥中心のものに近いことが分かった。このように CdTe 検出器に対する高速中性子の影響とその原因が本研究で初めて明らかになった。

次に CdTe 検出器に対する重水素イオン注入の効果を調べた。低線量で重水素注入された検出器では電子移動度のわずかな上昇が観測された。この結果が

ら注入された重水素原子により CdTe 結晶中の固有の欠陥が不活性化されることが示された。対照的に高線量の照射では著しい移動度の低下が観測された。過剰な重水素注入は検出器性能の低下を引き起こすことが分かった。

最後に CdTe 検出器の高エネルギー γ 線領域における応答特性の改善に高速中性子の照射効果を利用することを提案し、実験的にその有効性を実証した。照射処理によって電子キャリアと正孔キャリアの輸送特性の差が小さくなることで、検出器の応答特性に関して放射線相互作用位置の違いによるパルス波高の揺らぎが著しく減少することが分かった。この結果、照射処理を施すと高エネルギー γ 線に対してエネルギー分解能が向上することが明らかになった。特に照射処理された検出器と立ち上がり時間弁別の信号処理との組み合わせによって、エネルギー分解能がさらに向上することが実験的に証明された。この一連の実験によって高速中性子照射効果を CdTe 検出器のエネルギー分解能の向上に応用できることが初めて実証された。

Contents

Chapter 1 Introduction	1
1.1 Background	1
1.2 Purpose of This Study	2
References	
Chapter 2 Overview of CdTe Detectors	5
2.1 Detector Characteristics	6
2.2 Spectroscopic Performance	9
2.3 Signal Processing of Rise Time Discrimination	11
2.4 Application of RTD Processing to CdTe Detectors	11
2.5 Measurement System with RTD Processing	14
2.6 Application of Two-dimensional Spectrum Analysis to Examination of Radiation Effects	16
References	
Chapter 3 Influence of Fast Neutron Irradiation	19
3.1 Introduction	20
3.2 Experimental	20
3.3 Results and Discussions	22
3.3.1 Spectroscopic Performance	22
3.3.2 Two-dimensional Spectrum Analysis	24
3.3.3 Pulse Height Spectrum of ¹³⁷ Cs with Different Rise Time	26
3.3.4 Carrier Mobility and Lifetime	26
3.3.5 Comparison with Gamma-ray Irradiation	29
3.3.6 Annealing Experiment	32
3.3.7 TSC Analysis	35
3.4 Conclusion	38
References	

Chapter 4	Effects of Deuterium Ion Implantation on Carrier Transport Property of CdTe Detectors	41
4.1	Introduction	42
4.2	Experimental Setup	42
4.3	Deuterium Ion Implantation	44
4.3.1	Measurement of 5.5 MeV α Particles	44
4.3.2	Spectroscopic Performance	49
4.3.3	Carrier Mobility	50
4.3.4	Polarization Effect	51
4.4	Conclusion	52
	References	
Chapter 5	Improvement of Radiation Response Characteristic on CdTe Detectors using Fast Neutron Irradiation	55
5.1	Introduction	56
5.2	Principle	56
5.3	Experimental Procedure	61
5.4	Results and Discussions	62
5.4.1	Detector Characteristics	62
5.4.2	Spectroscopic Performance for High-energy Photons	64
5.4.3	Performance with RTD Processing System	66
5.4.4	Performance Stability	70
5.5	Conclusion	70
	References	
Chapter 6	Summary	73
	Appendix	75
	Acknowledgements	77
	List of Publications	78

Chapter 1

Introduction

1.1 Background

Cadmium telluride (CdTe) has been focused as a promising material for a room temperature X-ray detector and its chemical and electrical properties were well studied⁽¹⁾⁻⁽³⁾. However, application of this detector has been unfortunately delayed due to several difficulties such as carrier trapping and polarization effect⁽⁴⁾⁽⁵⁾ for a long period. Although, a lot of efforts were devoted to improve the material property, the quality of a CdTe crystal was not enough for reliable operation. In recent years, performance of the CdTe detector has been significantly improved by the modern technology of crystal growth⁽⁶⁾⁻⁽⁸⁾. Due to this, industrial products were made with various types⁽⁹⁾⁻⁽¹⁰⁾. The CdTe detectors are successfully used in wider fields such as dosimetry, astrophysical research, medical analysis, and radiation imaging^{(11),(12),(13)}. Further development of this detector is now expected.

Comparing with germanium (Ge) or silicon (Si) based radiation detectors, the CdTe detector allows us to construct a relatively inexpensive and compact detection system owing to its ability of room temperature operation. Therefore this detector has a potential to be commonly utilized instead of Ge or Si detectors in the fields of advanced technologies; medicine, space, and nuclear domain⁽¹³⁾. When the field of the application is widely grown, the CdTe detector has an opportunity to be used in severe conditions such as in lower temperature, high humidity, or heavy radiation. In research or industrial application, the detector might be forced to encounter intense radiations; gamma rays, fast neutrons, high-energy particles, and electrons. Such radiations introduce numerous changes in the properties of a CdTe crystal, and therefore the performance of the irradiated detector becomes quite different from the original one.

Since sufficient experimental data of the radiation effects have not been collected for this new detector, the utilization of the CdTe detector is limited by uncertainty in its performance in the presence of heavy radiation field.

Understanding of the radiation effects in the CdTe detectors is of interest to many users who are forced to use the detector in severe radiation environments such as nuclear reactors, accelerators, and satellite experiments. For example, in future the CdTe detector will be used in a space environment for high resolution gamma-ray measurements from a satellite. However, the CdTe detector may be subjected to intense radiations which consists of high energetic protons, heavy ions, and cosmic rays. It is also important that fast neutrons are generated from the interaction of cosmic rays with structural materials in spacecrafts or satellites. In such a severe environment, radiation hardness is quite important for the performance stability and the reliability of the detector. Accordingly, progressive study of the radiation effects are required for further development of semiconductor-type radiation detectors.

1.2 Purpose of This Study

The purpose of this study is to examine the influence of radiations on the spectroscopic performance of the CdTe detector. This study also aims to clarify the relationship between the performance change and the characteristic of the defects generated by radiations. The contents of this study contribute not only the evaluation of radiation hardness of the CdTe detector but also the characterization of radiation defects in such a binary semiconductor material. For the CdTe detector, the study related with gamma-ray irradiation has been examined by a few researchers⁽¹⁴⁾, but the influence of fast neutrons and charged particles has never been reported to date. Fast neutrons and high-energy charged particles are characterized by their higher ability of defect creation. A lot of vacancies and atom interstitials, which condense in a small region of a bulk, are then generated by such radiations. In contrast, high-energy photons and electrons spend most of their energy on electric excitation and therefore defect creation associated with atom displacement can be regarded to be scarce. From this point, the detector performance is likely to be affected strongly by fast neutrons or charged particles rather than high-energy photons or electrons. Especially for fast

neutrons, these radiation defects distribute homogeneously to the whole volume because of higher transmission ability. The characteristic feature of the defects by fast neutrons is known to be quite different from that by high-energy photons. It is quite important to examine the effect of fast neutrons. For this reason, this thesis describes the effect of fast neutrons as a main content.

When the influence of charged particles is concerned, it seems rather complicated. If the energy of charged particles is low, the range of the injected particle becomes shorter, and then the region of defect creation is restricted to the surface of a CdTe crystal. Most of the detector response is not affected by the generated defects since the volume of the damaged region is quite smaller than the whole sensitive volume of the detector. However, the detector response is likely to change significantly when the radiation interaction position overlaps such a region. Additionally, chemical behavior of the injected particle affects the electrical property of the CdTe crystal. When high-energy protons are fully injected to the CdTe detector for instance, they diffuse as hydrogen atoms from the surface to the inside of the bulk. The hydrogen atoms interact with bulk elements, impurities, and intrinsic defects and consequently they change the electrical property of the detector. Consequently the detector performance depends not only on radiation defects localized at a specific region but also on the chemical behavior of the injected particles. The influence of charged particles on the CdTe detector is somewhat complex since it depends on particle energy, species, irradiation fluence, direction of the injection, and so on. Recently, the chemical behavior of hydrogen in CdTe has become an important subject of investigation. Several reports on the interaction of hydrogen with structural defects in CdTe have shown that a hydrogen atom is able to compensate certain defects. However, the relation is unclear between the performance of the CdTe detector and the electrical property of CdTe containing hydrogen or its isotope; deuterium (D). In this study, D ion implantation experiment was thus conducted to clarify the effects of both defects directly generated by D ions and the chemical property of the implanted deuterium atoms in CdTe.

The experimental results are described as follows. Background and the purpose of this study are described in this chapter. Chapter 2 describes the overview of the CdTe detector and explains the principle of rise time discrimination briefly. Radiation response characteristic is also introduced. Chapter 3 deals with the experimental

results of the influence of fast neutron irradiation. The results of deuterium ion implantation to the CdTe detector are described in Chapter 4. Chapter 5 contains the results of the performance enhancement by means of the fast neutron pre-irradiation. Application of fast neutron irradiation to improve detector performance is demonstrated in this Chapter. The final chapter as Chapter 6 summarizes the findings of this work.

References

1. Siffert, P. et. al., : Nucl. Instrum. Methods, 150, 31 (1978).
2. Mayer, J. W. : Nucl. Instrum. Methods, 43, 55 (1966).
3. Yee J. H. et al.,: IEEE trans. on Nucl. Sci. Vol. NS-23, No. 1, 117 (1976).
4. Siffert, P. et. al.,: IEEE trans. on Nucl. Sci. Vol. NS-23, No. 1, 159 (1976).
5. Zanio K. R. et. al.,: J. Appl. Phys., Vol. 39, No 6, 2818 (1968).
6. Shoji, T. et. al.,: Nucl. Instrum. Methods, Phys. Res., A322, 324 (1992).
7. Mergui, S. et. al., : Nucl. Instrum. Methods, Phys. Res., A322, 375 (1992).
8. Shoji, T. et. al.,: IEEE trans. on Nucl. Sci. vol 40, No. 4, 405 (1993).
9. Iwase, Y. et. al.,: Nucl. Instrum. Methods, Phys. Res., A322, 628 (1992).
10. Baba, S. et. al.,: ITE Technical Report, Vol. 21, No. 32, 19 (1997).
11. Squillante, M. R. and Entine, G. : Nucl. Instrum. Methods, Phys. Res., A322, 569 (1992).
12. Scheiber, C. and Chambron, J.,: Nucl. Instrum. Methods, Phys. Res., A322, 604 (1992).
13. Arlt, R. et. al.,: Nucl. Instrum. Methods, Phys. Res., A322, 575 (1992).
14. Taguchi, T. et. al.,: Nucl. Instrum. Methods., 150, 43 (1978).

Chapter 2

Overview of CdTe Detectors

This chapter briefly describes overview of a CdTe detector and principle of rise time discrimination (RTD) processing. The experimental setup for the RTD processing is also explained. Application of the RTD processing to the analysis of radiation effect is proposed in this chapter⁽¹⁾⁻⁽⁴⁾.

2.1 Detector Characteristics

A CdTe detector has advantageous properties such as higher detection efficiency, room temperature operation and higher resolving power for low energy photons. The characteristic of this detector is based on the material property of a CdTe; large atomic number, a wide bandgap, and higher resistivity. Table 2.1 compares the material property for typical radiation detectors. For the CdTe detector, the average value of the atomic number (Z) becomes 50 and is well situated for detecting photoelectric interaction events effectively. Compared with Si ($Z=14$) or Ge (32) detectors, a peak to Compton ratio becomes much higher for the CdTe detector since the cross-section of the photoelectric interaction follows the factor of Z^n ($4 < n < 5$). Figure 2.1 presents linear attenuation coefficient for photoelectric absorption, Compton scattering and pair production. The CdTe detector is expected to provide higher detection efficiency for lower-energy photons around 100 keV rather than other detectors. Additionally, the wider bandgap of the CdTe enables the room temperature operation and this characteristic makes the detector more attractive for various fields of application. Although excessively large bandgap decreases the number of electron-hole pairs oppositely, the gap energy of 1.54 keV is better for room temperature operation with low thermal noise.

Table 2.1 The properties of the materials promising for radiation detectors.

	Bandgap Energy (eV) at 300K	Atomic Number (Z)	Pair Creation Energy (eV)	Electron Mobility (cm^2/Vs)	Hole Mobility (cm^2/Vs)	Electron Lifetime (μs)	Hole Lifetime (μs)
CdTe	1.54	48-52	4.43	1000	80	1	1
Si	1.12	14	3.61	1500	600	3000	3000
Ge	0.67	32	2.96	3900	1800	1000	1000
HgI	2.1	53-80	4.15	100	4	0.1	0.01

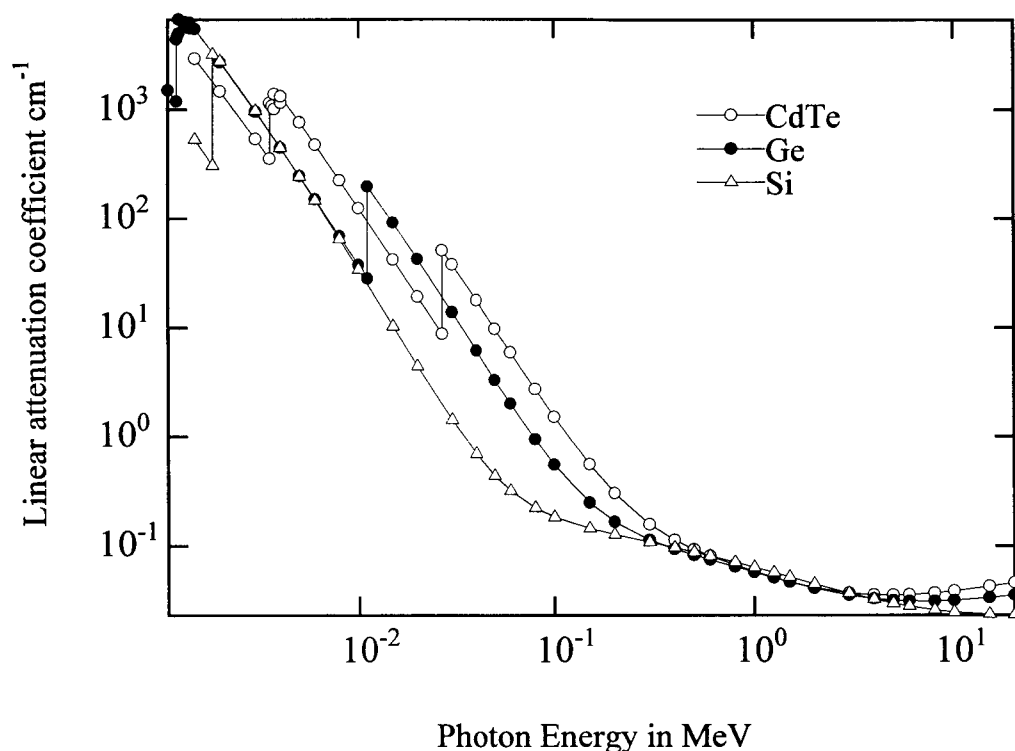
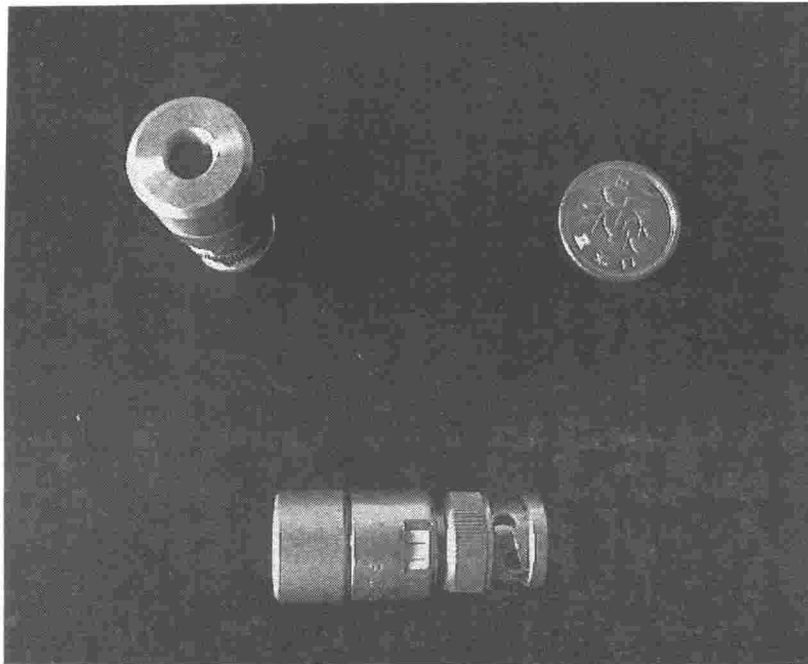


Fig. 2.1 Attenuation coefficient for different materials as a function of photon energy. Only photoelectric attenuation is presented.

Figure 2.2 shows the commercial planar-type CdTe detectors (CD2BE, Toyo Medic Co.). Close view of the sensor part is also shown in the window. The physical dimensions of this detector is 4 cm in length and 1.5 cm in diameter. The volume of the CdTe crystal is approximately 3.2 mm^3 ($2 \times 2 \times 0.8 \text{ mm}$). In conventional use, a beryllium thin window is attached to the front side of the detector to reduce the attenuation of incident radiation. A BNC-type connector is integrated in the detector to decrease electromagnetic noise. Cross-sectional view of the sensor part is illustrated in Fig. 2.3. The CdTe crystal is mounted in an aluminum cell and thin gold wires are attached to the both sides of the crystal for applying the bias. This structure is popularly used for commercial CdTe detectors. Other types of the CdTe detectors are reported in Ref. 5 and the details are not described here.

(a)



(b)

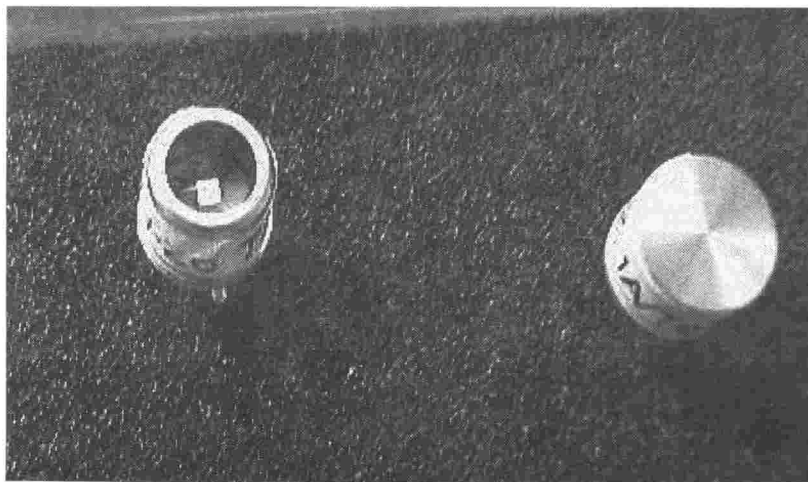


Fig. 2.2 Planar-type CdTe detectors
(a) Front and side view
(b) Close view of the sensor part

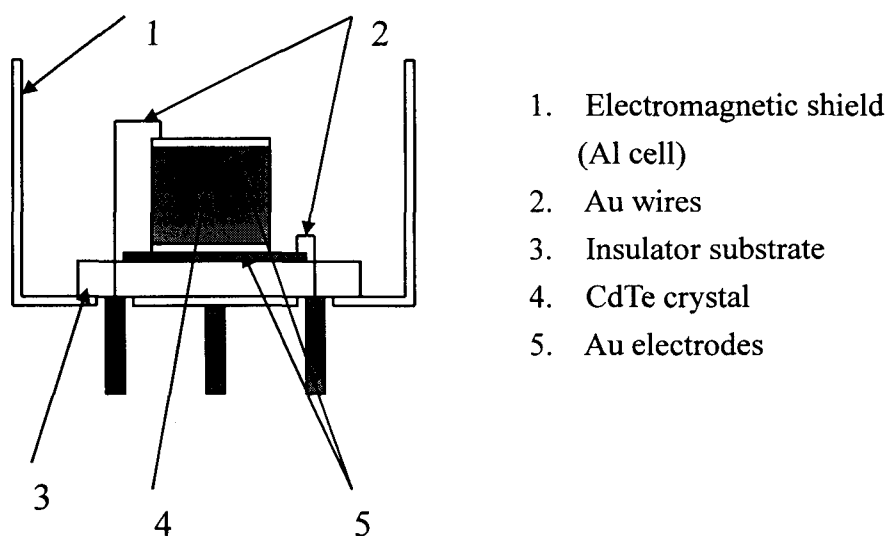


Fig. 2.3 Cross-sectional illustration of the sensor part.

2.2 Spectroscopic Performance

Figure 2.4 shows representative pulse height spectra measured with the CdTe detector by the author. The spectra of ^{241}Am (a), ^{133}Ba (b) and ^{137}Cs (c) are presented respectively. The CdTe detector provides better energy resolution for lower-energy photons. Actually, the full width at half maximum (FWHM) at 59.5 keV reaches to be approximately 3.8 keV. On the other hand the full energy peak of 662 keV becomes broader due to peak tailing to lower channels as indicated in Fig. 2.4(c). This peak tailing results from the hole collection loss. The small mobility of the hole is an intrinsic characteristic of CdTe as shown in Table 1. Thus the hole collection loss becomes a serious problem for improving the detector performance.

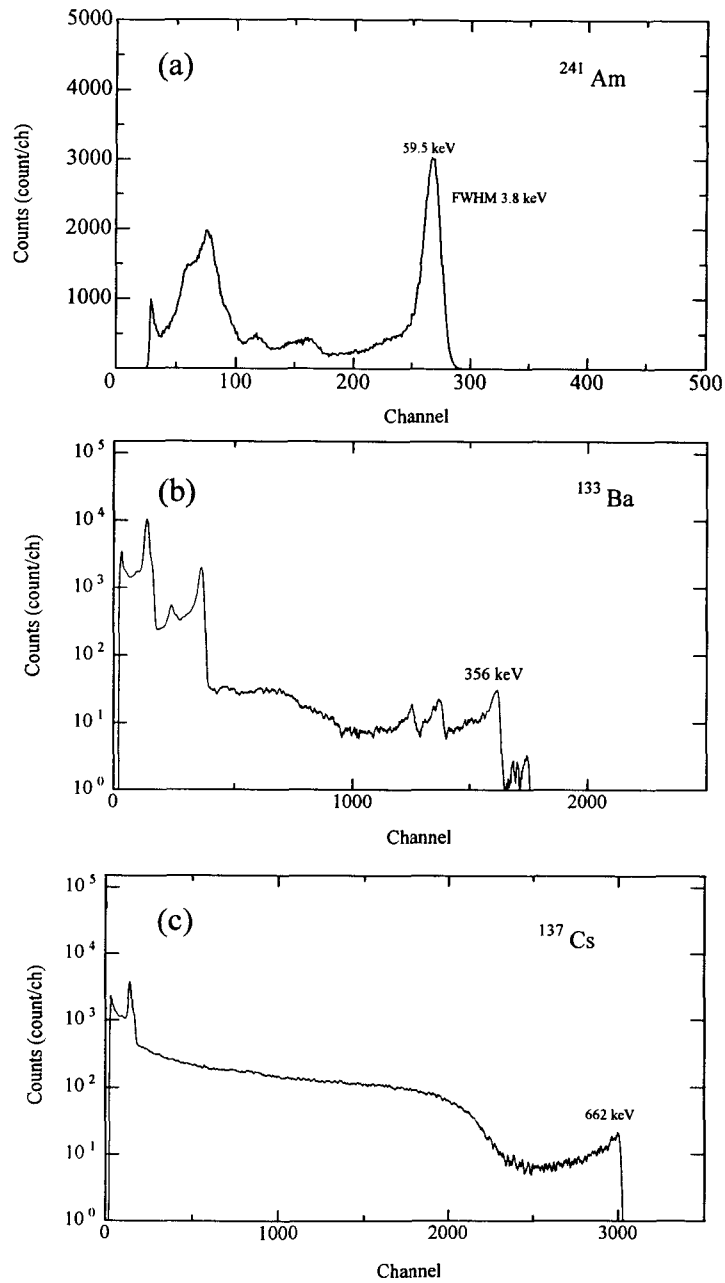


Fig. 2.4 Pulse height spectrum of each ^{241}Am (a), ^{133}Ba (b), and ^{137}Cs (c).

2.3 Signal Processing of Rise Time Discrimination

Rise time discrimination (RTD) is electronic signal processing, in which a radiation pulse is classified by its rise time and only specific pulse is selected for spectrum formation. This method is almost the same as pulse shape discrimination (PSD), which is commonly used to distinguish fast neutrons from gamma rays in the response of a scintillation detector. On the RTD processing, the rise time of every radiation pulse from the detector is measured by an additional electronic instrument introduced to a conventional detection system. The information of the obtained rise time is referred and used to collect the pulse whose rise time satisfies selection criterion. The RTD processing is not applicable when each pulse exhibits almost the same rise time; as is the case for the response of a charged particle on a surface-barrier detector. However, this processing becomes effective in various purposes (e.g. the separation of radiation species, the reduction of detector noise and the improvement of energy resolution for the radiation detectors).

2.4 Application of RTD Processing to CdTe Detectors

The RTD processing is commonly used to improve the energy resolution of the CdTe detector. For the planar-type CdTe detector, the response pulse of a high-energy gamma ray exhibits characteristic feature as shown in Fig. 2.5, in which typical response pulses for 662 keV gamma rays are presented. Although these pulses originate from the same energy deposition of the gamma ray, the shape of each response pulse shows large difference. Figure 2.6 shows the schematic diagram of the CdTe detector response. When the radiation deposits its energy near the negative electrode side, the motion of the generated electrons becomes major for pulse formation since the holes are collected quickly to the negative contact. Due to higher mobility of the electrons, the carrier collection time becomes much shorter, and then the pulse amplitude shows steep increase in time like the pulse (a) which provides the shortest rise time in the figure. In the case when the interaction position locates in the middle of the CdTe crystal, both carriers contribute pulse formation equally. However, the rise time of this pulse becomes longer because of smaller mobility of the holes.

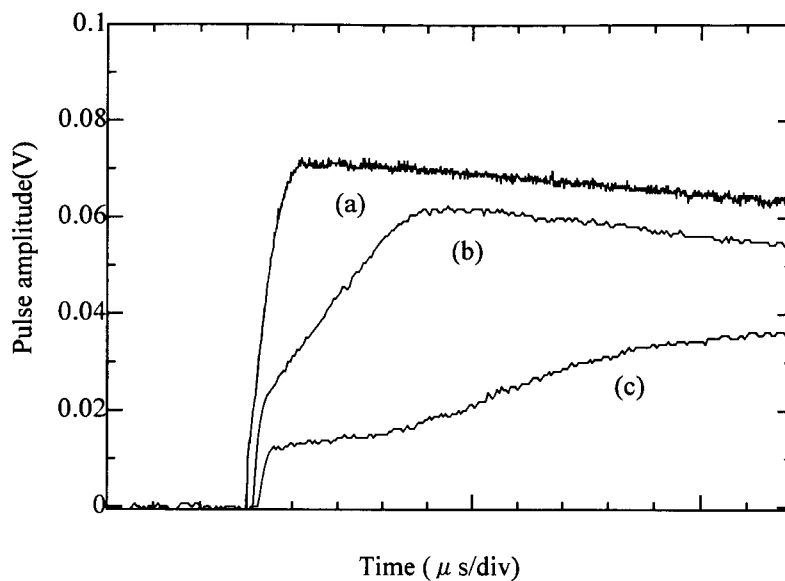


Fig. 2.5 Voltage pulses acquired from the planar-type CdTe detector.

Additionally, the small hole mobility induces charge collection loss, and therefore the amplitude of this pulse becomes smaller than that of the shortest rise time pulse. In this way the pulse amplitude changes when the interaction position differs. This response characteristic of the CdTe detector causes the fluctuation of pulse amplitude and leads to poor energy resolution on the measurement of high-energy photons. For the CdTe detector, the RTD processing is commonly employed to collect only shorter rise time pulses. The influence of the collection loss can be suppressed by discarding the longer rise time pulses. Due to this, the combining the CdTe detector with the RTD processing exhibits good energy resolution. The resolution enhancement using the RTD processing is reported in Refs. 6 and 7.

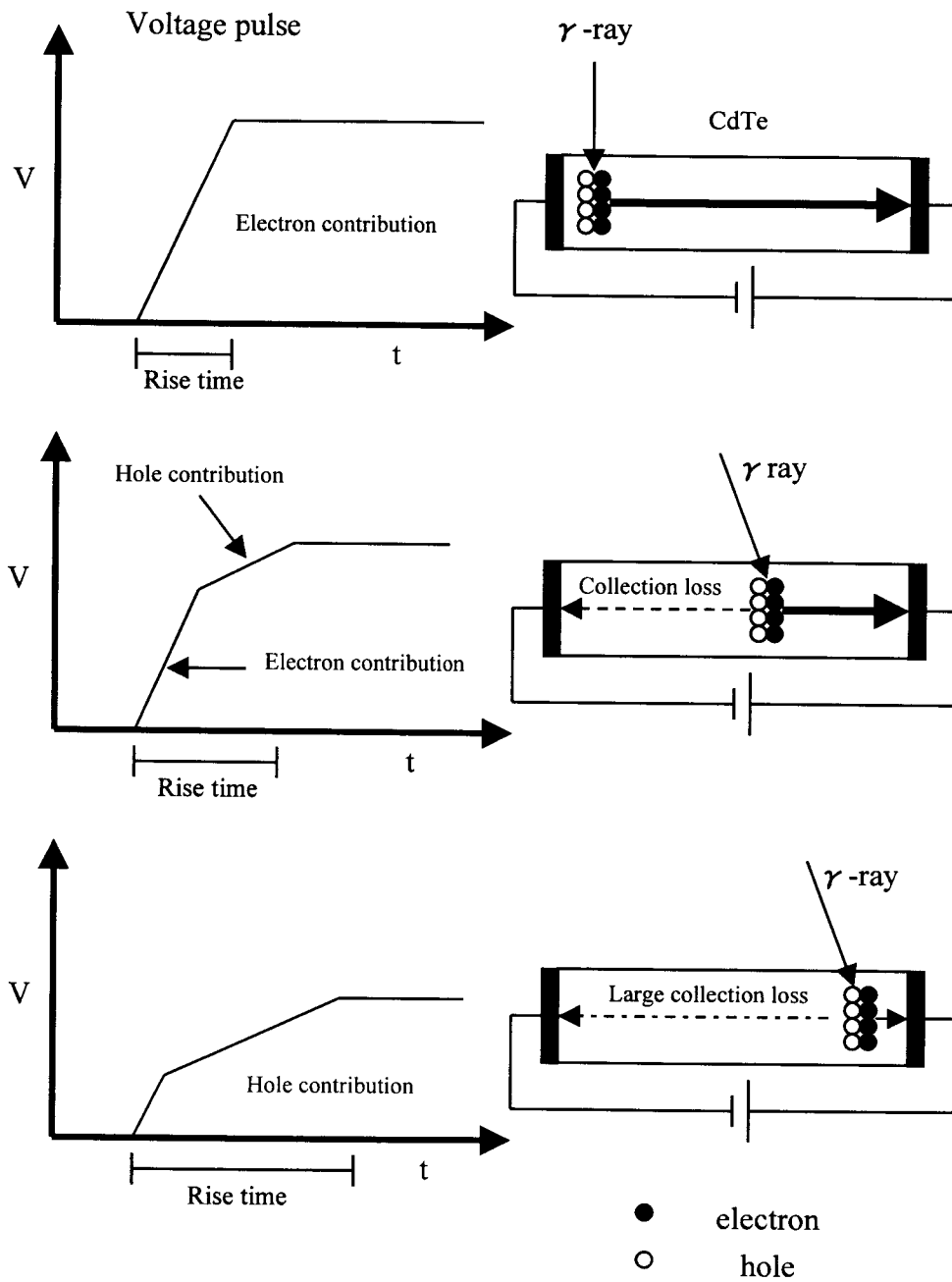


Fig. 2.6 Schematic illustration of the detector response.

2.5 Measurement System with RTD Processing

The block diagram of the measurement system used throughout this study is shown in Fig. 2.7. This represents a typical RTD processing system consisted of standard NIM modules. The charge generated in the detector is amplified in the preamplifier. A detector pulse is branched in two paths: first to a multimode amplifier for pulse height measurement, while the second path is the system for rise time analysis. On the rise time measurement path, a timing filter amplifier is used to amplify the pulse from the preamplifier and the instrument of dual sum and invert is used to change the polarity of the pulse. With a constant-fraction discriminator, a "Start" signal is generated on the edge of the pulse and a "Stop" signal is generated on the edge of 90 % pulse amplitude with a pulse-shape analyzer. The time interval between two timing signals, corresponding to a pulse rise time, is converted into voltage with a Time-to-Amplitude Converter (TAC). By adjusting the upper and lower limits of the voltage, acceptable rise time width can be set. When the pulse within the set rise time width is introduced to the TAC, the TAC outputs one voltage pulse. This pulse is subsequently fed into a linear gate and used to gate the pulse height measurement path to select the pulse with right rise time. Finally, the pulse height spectrum is formed from the selected pulses since the pulses with the rise time exceeding the set rise time width are inhibited at the gate. This is a procedure of the RTD processing system.

The dotted lines in the figure represent the paths for two-dimensional spectrum analysis. The pulse amplitude signal is delayed with a delay amplifier and both rise time and amplitude signals are introduced to a coincidence unit consisting of two analog-to-digital converters at the same timing. From the outputs of the unit, a two-dimensional (amplitude- rise time) spectrum is constructed with a personal computer.

Figure 2.8 shows pulse rise time distribution of 1mm thick CdTe detector. This distribution was experimentally taken by measuring ^{137}Cs gamma rays. The pulse count at the short rise time becomes much higher than that for longer rise time. However, this distribution represents typical response profile of the planar-type CdTe detector.

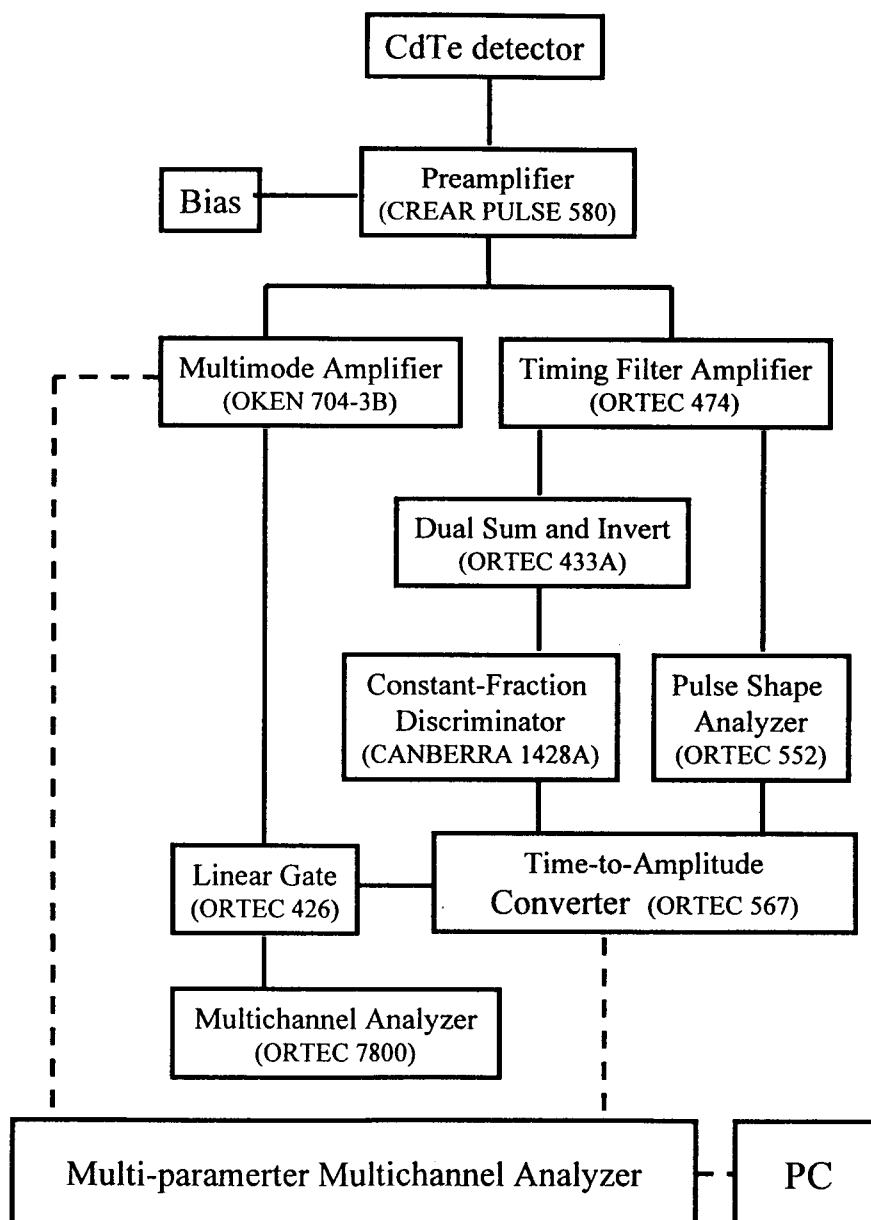


Fig. 2.7 The detection system with RTD processing.

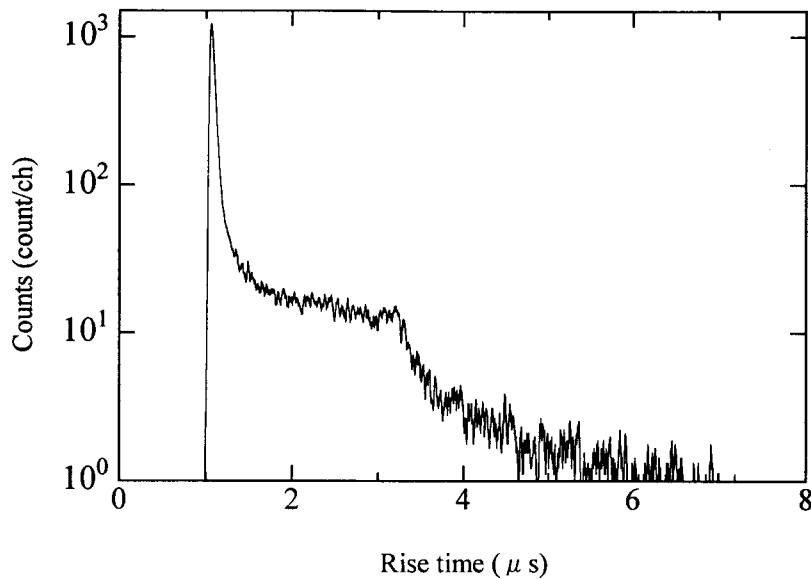


Fig. 2.8 Pulse rise time distribution of the CdTe detector for the response of ^{137}Cs .

2.6 Application of Two-dimensional Spectrum Analysis to Examination of Radiation Effects

The simultaneous measurement of the pulse amplitude and the rise time provides further information about the response characteristic of the detector. Figure 2.9 exhibits the two-dimensional spectrum of ^{137}Cs measured with the CdTe detector. The difference of counting ratio is expressed as a contour in this figure. One can see that the rise time distributes approximately from $0.4\ \mu\text{s}$ to $5\ \mu\text{s}$. The pulse distribution of the 662 keV photopeak is clearly shown as a contour locating around 600 keV. The large contour below the photopeak distribution corresponds to the continuum of the Compton effect. As indicated in the figure, the position of the photopeak moves to the lower energy side with increasing the rise time. This is due to the charge collection loss originated from the smaller mobility of the hole. The motion of the electrons is responsible for the pulse distribution at the shorter rise time, while the distribution locating at the longer rise time is composed from the motion of the holes. Hence the

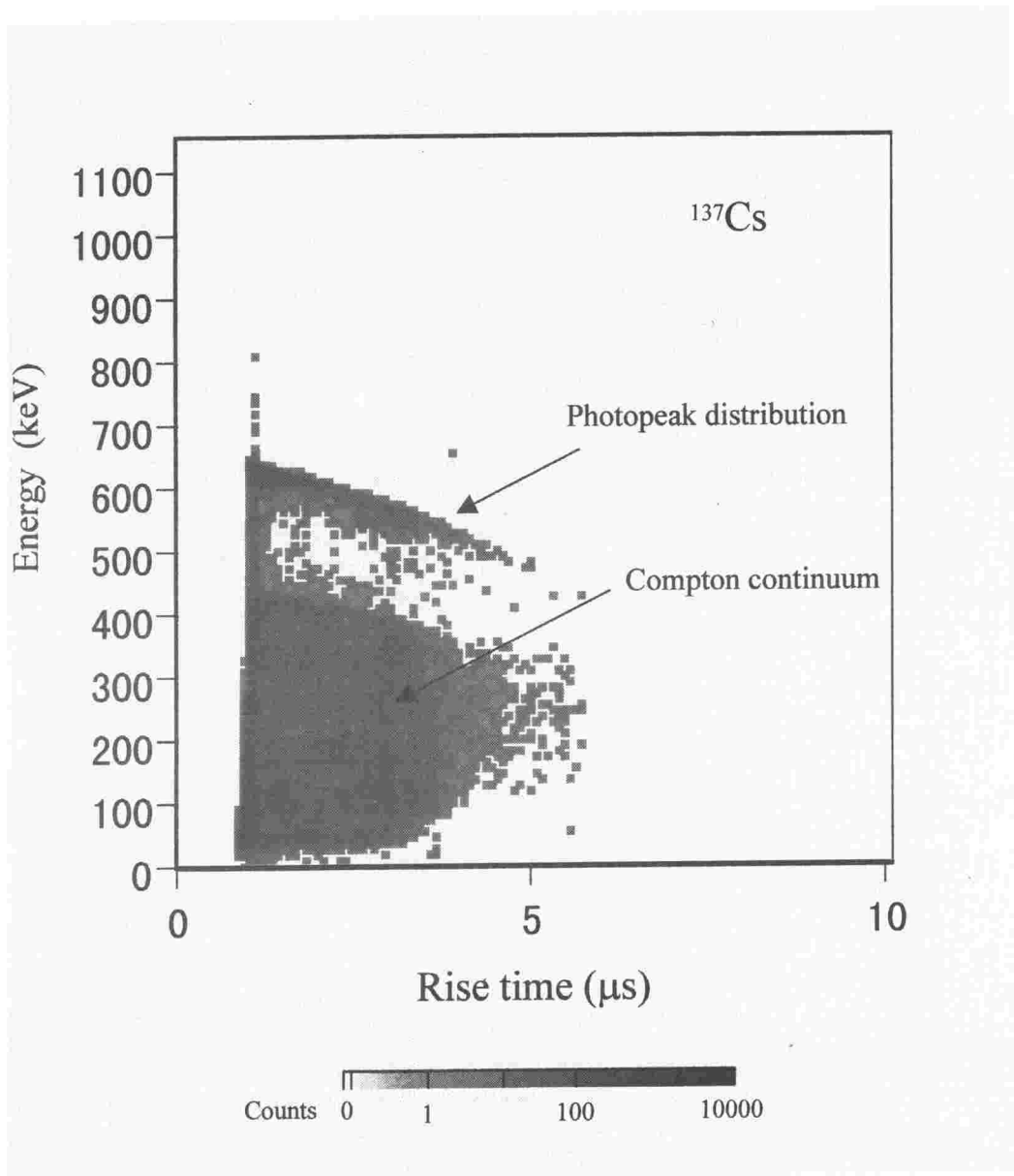


Fig. 2.9 Two-dimensional spectrum of ^{137}Cs measured with the CdTe detector.

transport property of the individual carrier can be examined independently by analyzing the two-dimensional spectrum. From this point, the two-dimensional spectrum analysis becomes an effective method to examine the radiation irradiation effect of the CdTe detector. Assume that radiation damage decreases the mobility for the holes but not for the electrons. At that time, the detector performance will degrade, and then the damaged detector will show a different shape of the pulse height spectrum comparing with the original. However the reason for performance degradation cannot be clarified only from the change of the pulse height spectrum. On the other hand, the carrier collection time can be evaluated from the two-dimensional spectrum. In this case, the pulse distribution at longer rise time changes its position to the direction of further long rise time since the hole mobility changes to be lower. Therefore the two-dimensional pulse distribution provides important information about the change of the carrier mobility.

In this study, the two-dimensional spectrum analysis is employed as a new method to examine the irradiation effect of the CdTe detector. Effectiveness of this method is presented in the following chapter.

References

1. H. Miyamaru, K. Fujii, T. Iida, and A. Takahashi, : J. Nucl. Sci. and Tech., Vol. 35, No.9, 679 (1998).
2. H. Miyamaru, K. Fujii, T. Iida, A. Takahashi, : J. Nucl. Sci. and Tech., Vol. 34, No.8, 755 (1997).
3. H. Miyamaru, K. Fujii, T. Iida, A. Takahashi, : J. Nucl. Sci. and Tech., Vol. 33, No.9, 744 (1996).
4. H. Miyamaru, K. Fujii, T. Iida, A. Takahashi, : *Ionizing radiation*, Vol.22, No. 3 43 (1996).
5. Schlesinger, T. E. and James, R. B.: "Semiconductors for Room Temperature Nuclear Detector Applications", Academic Press, Vol. 43, New York, (1995).
6. Richter, M. and Siffert, P.: Nucl. Instrum. Methods, Phys. Res., A322, 529 (1992).
7. Ivanov, V. I. et. al.,: IEEE trans. on Nucl. Sci. Vol 42, No. 4, 258 (1995).

Chapter 3

Influence of Fast Neutron Irradiation

The influence of fast neutron irradiation on a planar-type CdTe detector was studied⁽¹⁾⁻⁽³⁾. The detector was irradiated with fast neutrons in the fluence range 1.0×10^8 - 1.8×10^{11} n/cm² and its spectroscopic performance was examined at several stages in the range. The effect of gamma-ray heavy irradiation toward the detector was also investigated for comparison. The gamma rays from ²⁴¹Am and ¹³⁷Cs standard sources were measured with the fast neutron-irradiated (n-irradiated) detector to examine the change of the response characteristic. Pulse amplitude and rise time for a response pulse were also measured using the RTD processing to construct a two-dimensional spectrum. The transport properties of both electrons and holes were evaluated individually. For the n-irradiated detector, the electron collection loss was apparently observed from the change of the spectrum shape of ²⁴¹Am. Electron lifetime in the n-irradiated CdTe significantly decreased with increasing the neutron fluence, while the one for the hole remained almost unchanged. The two-dimensional spectrum of ¹³⁷Cs also indicated that deep electron-trapping centers were generated by the fast neutrons and they degraded the detector performance.

To assign the electron-trapping center by fast neutron irradiation, isochronal annealing and thermally stimulated current (TSC) analysis were carried out for the n-irradiated CdTe. Experimental results clarified that the electron-trapping center is associated with a Cd vacancy or an interstitial.

3.1 Introduction

Nowadays, the development of crystal growth technique allows the production of a large CdTe crystal with high purity. The modern technology directly contributes to the improvement of detection efficiency and energy resolution for the CdTe detectors⁽⁴⁾. However, despite the considerable progress made in material development, the spectroscopic performance still depends on the concentration of structural defects, impurities and their combinations in the CdTe crystal⁽⁵⁾. These defects become the origin of carrier collection loss or polarization effect, resulting in poor detector performance. Thus the defect concentration is a serious problem for further development. As well known, electronic and atomic defects generated by radiation also affect the detector performance⁽⁶⁾. Radiation-induced defects also affect not only spectroscopic performance but also performance stability of the detector. Radiation hardness of the CdTe detector is quite important when used in severe radiation environments (e.g. X-ray imaging, radiation monitoring in nuclear power plants, and astrophysical survey in spacecrafts). The change of the response characteristic has been reported for the CdTe detector irradiated with gamma-rays⁽⁷⁾. The influence of the gamma rays and electrons were well examined⁽⁸⁾, but quite a few results have been reported about the influence of fast neutrons until now. Therefore this study was aimed to obtain the experimental data of the influence of fast neutron irradiation on the CdTe detector. Performance change due to the irradiation was monitored as a function of neutron fluence. The mechanism of the performance change is discussed in relation with the characteristics of the defect generated by fast neutrons.

3.2 Experimental

A CdTe specimen was grown by the traveling heater method (THM) with six nines purity. The dimensions of the specimen were 2.0 mm length, 1.8 mm width and 0.8 mm thickness. Thin gold deposition with 200 nm was applied on both sides of the specimen to form electric contacts. A planar-type CdTe detector was fabricated with this specimen. Two detectors were prepared to compare different irradiation conditions; fast neutron irradiation (1) and gamma-ray heavy irradiation (2). Both

detectors were confirmed to show almost the same spectroscopic performance before irradiation. One of the two detectors was irradiated with 14MeV fast neutrons generated by the deuteron accelerator OKTAVIAN⁽⁹⁾. The detector was irradiated in the fluence range $1.0 \times 10^8 - 1.8 \times 10^{11}$ n/cm². At several stages in the fluence range, the detector was taken out from an irradiation apparatus and its spectroscopic performance was evaluated by measuring ²⁴¹Am and ¹³⁷Cs gamma rays. Heavy irradiation with gamma rays (⁶⁰Co gamma rays, 500 Gy) was performed against the rest of the detectors. The performance was also examined with the same manner.

The system for measuring a pulse height spectrum consisted of a preamplifier (CLEAR PULSE 656), a spectroscopy amplifier (ORTEC 543), and a multi-channel analyzer (ORTEC 7800). The detector was operated with the voltage of 50V (417 V/cm). All measurements were conducted at room temperature. A two-dimensional spectrum was also acquired from the RTD processing described in Chapter 2 for detailed examination of the irradiation effect. Pulse shaping time of the spectroscopy amplifier was set to be 5 μ s. Pulse rise time was calibrated with a precision time calibrator (ORTEC 462). In order to evaluate carrier mobility and lifetime, the shape of a gamma-ray pulse was directly measured and stored with a fast digital oscilloscope (LeCroy 9384). From the rise time obtained from the pulse shape, the transit time of each carrier was evaluated. The carrier mobility was calculated from the experimental data of the transit time, the detector thickness, and the amplitude of the bias voltage. To evaluate the carrier lifetime, the stored pulse shapes were analyzed with the Hecht relation⁽¹⁰⁾ as,

$$V(t) = \frac{Q_o \cdot E}{C \cdot d} \left[\mu_e \tau_e \left\{ 1 - \exp\left(\frac{-t}{\tau_e}\right) \right\} + \mu_h \tau_h \left\{ 1 - \exp\left(\frac{-t}{\tau_h}\right) \right\} \right]$$

where Q_o : Total charge generated by radiation

E : Amplitude of applied electric field

C : Device capacitance

d : The distance between two electrodes

μ_e, μ_h : Carrier mobility for electrons and holes

τ_e, τ_h : Lifetime for the individual carrier.

3.3 Results and Discussions

3.3.1 Spectroscopic Performance

Figure 3.1 shows a series of ^{241}Am spectra measured with the n-irradiated CdTe detector. The detector was subjected to the gamma rays from the negative contact side. In this condition, 50 % of 59.5 keV gamma rays are attenuated within about 150 μm from the negative contact because of the large attenuation coefficient of CdTe. Therefore, electron-hole pairs are mostly generated nearby the negative contact side. The generated holes are collected quickly to the negative contact, and then its drift length becomes much shorter than that of the electrons. At that time the radiation pulse is formed mostly by the motion of the electrons rather than that of the holes⁽¹¹⁾. Consequently, the change of the spectrum shape originates from the one of the electron transport property. As shown in the figure, the main photopeak moves gradually toward lower channels with increasing the fluence. The full width at half maximum (FWHM) for the photopeak is 4 keV before irradiating and it changes to be 13 keV after the irradiation of $1.5 \times 10^{10} \text{ n/cm}^2$.

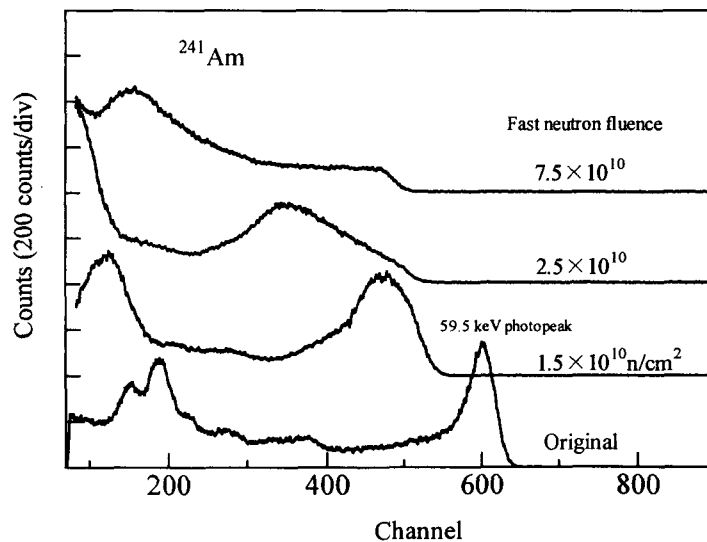


Fig. 3.1 ^{241}Am gamma-ray spectra measured with the CdTe detector irradiated with fast neutrons. The detector is subjected to the gamma-rays from the negative contact side.

Next, the detector was subjected from the positive contact side. In this case, the holes become major for the pulse formation. The pulse height spectra were taken as indicated in Fig. 3.2. When we compare the initial position of the main photopeak for both subsection conditions, the one for the injection from the positive side locates at approximately 25 % lower. This can be explained due to the hole trapping caused by intrinsic defects. This trapping effect results in poor collection of the holes and therefore the pulse amplitude becomes smaller. As a consequence, the photopeak appears at the lower channels rather than that for the case of electron collection. As far as the neutron fluence is below 5.0×10^{10} n/cm², the change of the spectrum shape was not observed. However, the peak position gradually moved to lower channels over the fluence of 7.5×10^{10} n/cm². The energy resolution does not change so significantly.

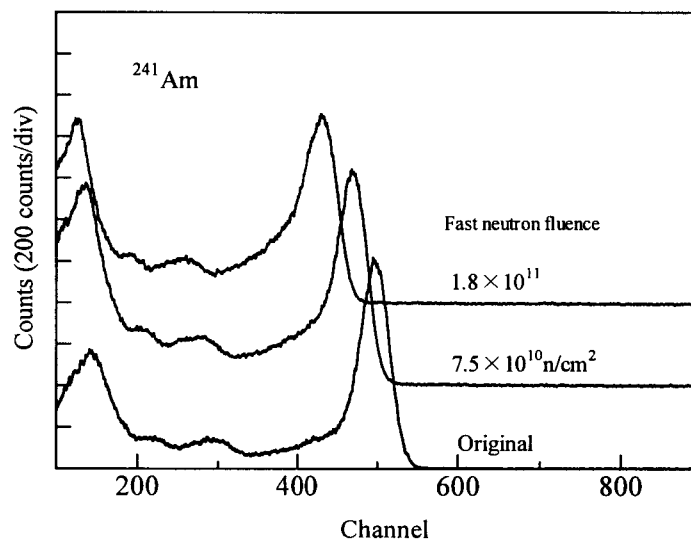


Fig. 3.2 ²⁴¹Am gamma-ray spectra for the n-irradiated CdTe detector. The detector is subjected from the positive contact side.

Figure 3.3 summarizes the carrier collection efficiency versus fast neutron fluence. The efficiency at each fluence was normalized against the one measured before neutron irradiation. The electron collection efficiency markedly decreases over the fluence of

$1.0 \times 10^{10} \text{ n/cm}^2$. On the other hand, the decreasing of the efficiency is quite small for the holes. This result indicates that the fast neutron irradiation reduces the collection efficiency of the electrons.

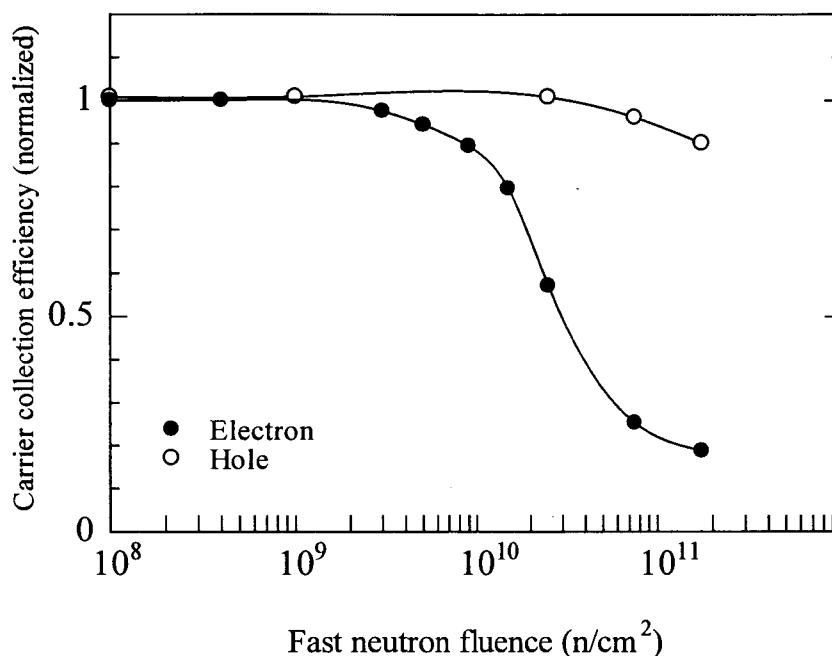


Fig. 3.3 Carrier collection efficiency for the n-irradiated CdTe detector.

3.3.2 Two-dimensional Spectrum Analysis

Two-dimensional spectrum analysis was employed to clarify the characteristic of the n-irradiated CdTe detector. Since high energetic gamma rays generate large pulses with better signal-to-noise ratio, ^{137}Cs gamma rays ($\sim 660 \text{ keV}$) were selected and used to examine the response characteristic of the detector. The detector was subjected with the gamma rays from the negative contact side. Figure 3.4 shows the two-dimensional (amplitude - rise time) spectrum of ^{137}Cs measured with the n-irradiated detector. The profile of the two-dimensional spectrum is presented as a function of fast neutron fluence. The difference of the pulse count is expressed as a contour in this figure.

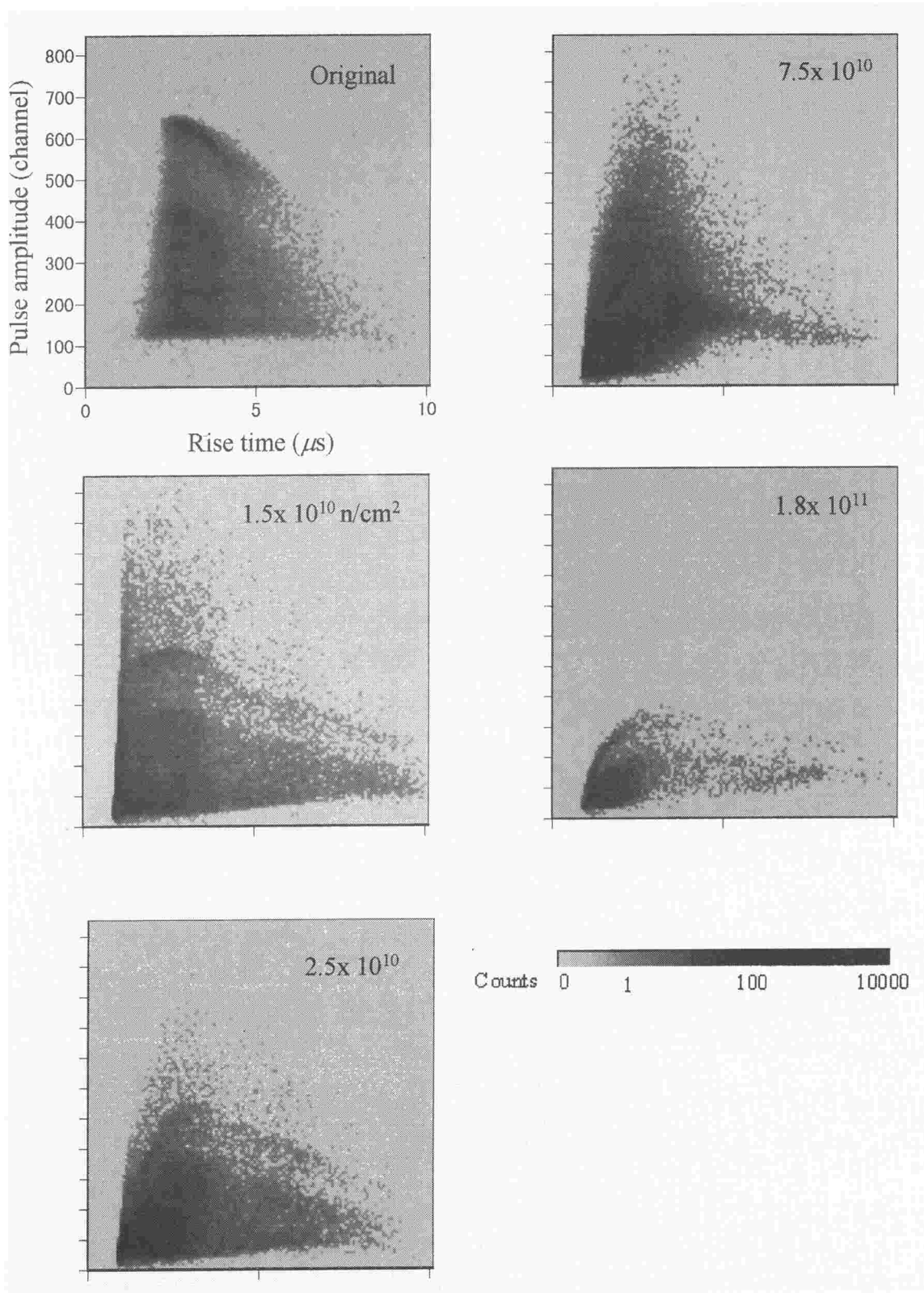


Fig. 3.4 Two-dimensional spectra of ^{137}Cs measured with the n-irradiated CdTe detector.

For the original, the pulse distribution corresponding to the response of the 662 keV gamma rays is clearly shown as a contour locating around 600 ch. As described in Chapter 2, the hole collection loss due to the intrinsic defects decreases the pulse amplitude. Therefore, the pulse distribution for the original falls right, but this is the intrinsic response characteristic of the CdTe detector. When neutron irradiation proceeds, the pulse distribution gradually moves its position to the smaller amplitude. Especially, the remarkable decreasing of the pulse amplitude can be seen at the shortest rise time. Since the motion of the electrons is responsible for the shorter rise time pulse, the change of the two-dimensional spectrum also suggests the reduction of the electron collection efficiency.

3.3.3 Pulse Height Spectrum of ^{137}Cs with Different Rise Time

The variation of the spectrum shape as a function of the rise time was examined by using the RTD processing. Each pulse was classified by the rise time width of every 1 μsec , and then the pulse height spectrum for different rise time was composed by taking the classified pulses in each rise time width. Accordingly this spectrum corresponds to the cross-sectional view of the two-dimensional spectrum at the specific rise time. The stacked plot of ^{137}Cs spectra is indicated in Fig. 3.5. Both spectra acquired from the original (a) and the n-irradiated detector (b) are compared. For the original, the position of the main photopeak (662 keV) shifts toward lower channels when the rise time becomes longer. This indicates that the shortest rise time pulse provides the largest pulse amplitude. On the contrary, the photopeak position shifts markedly toward lower channels in the spectrum of 0-1 μs when using the n-irradiated detector. The spectrum shape in the rise time width 0-2 μs changes significantly, but the peak positions for the rise time over 3 μs is almost the same as the original.

3.3.4 Carrier Mobility and Lifetime

In order to clarify the reason for the performance change, carrier mobilities and lifetimes for the n-irradiated CdTe were measured. The results are presented in each

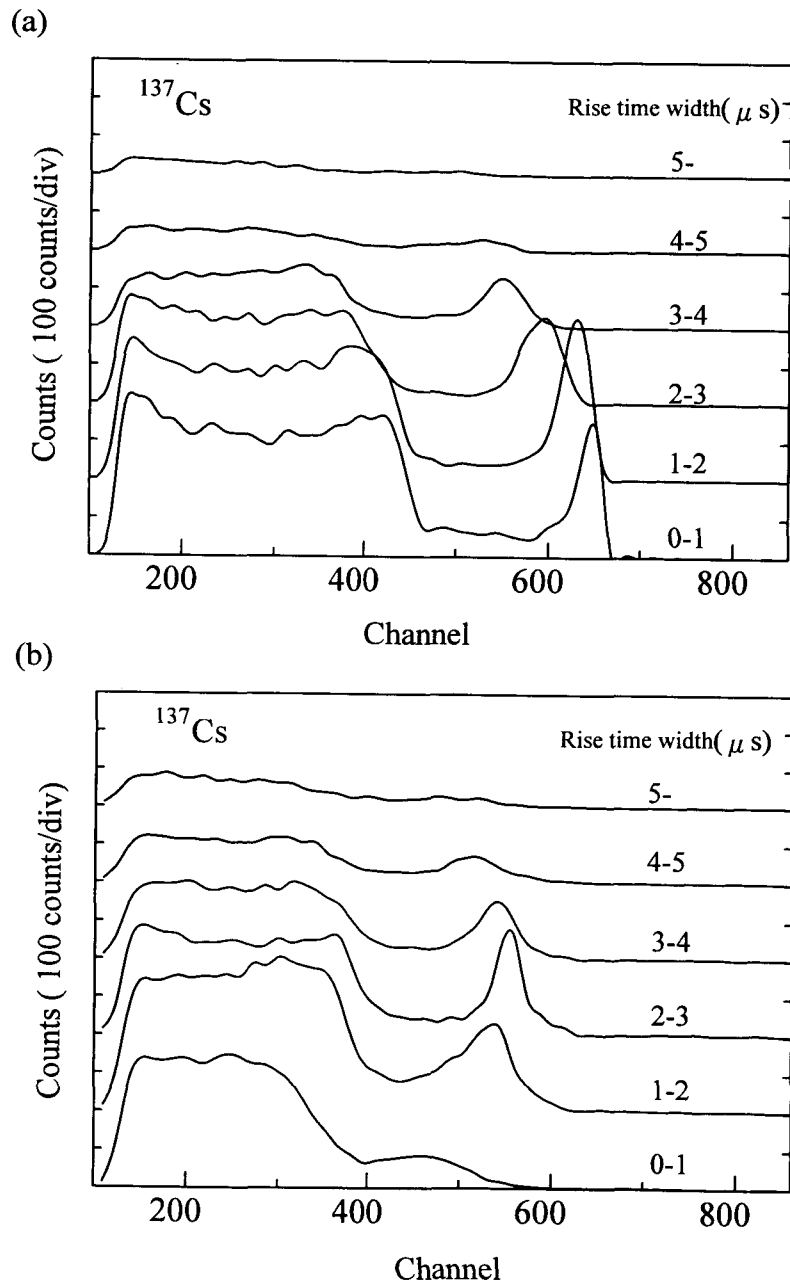


Fig. 3.5 ^{137}Cs gamma-ray spectra with different rise times; (a) the original (b) after the irradiation of $1.6 \times 10^{10} \text{ n/cm}^2$.

Fig. 3.6 and 3.7 as a function of fast neutron fluence. The electron mobility gradually decreases with increasing the fluence, but the one for the hole does not show any change. As for the carrier lifetimes, significant decrease is observed for the electron lifetime, whereas the hole lifetime remains almost unchanged. For the original, the lifetimes were $5.1 \mu\text{s}$ for electrons and $6.3 \mu\text{s}$ for holes. When the fluence reaches $4 \times 10^9 \text{ n/cm}^2$, the lifetimes become $1.1 \mu\text{s}$ (79 % decrease) and $6.2 \mu\text{s}$ for the individual carrier. It was clearly shown that the fast neutron irradiation affected the transport property of electrons rather than that of holes within the fluence of this study.

The experimental results indicated that the significant change of the electron transport property was caused by the fast neutron irradiation. It was also found that the property of the holes was almost unaffected. However, these results are not enough to clarify the origin of this irradiation effect. Additional experiments were undertaken to examine the defect generated by fast neutrons as followings.

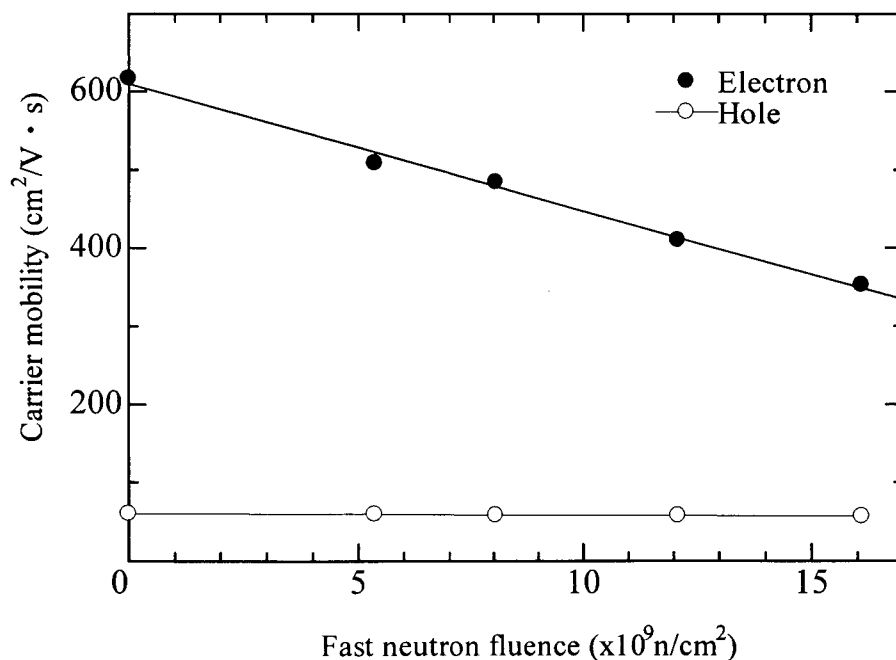


Fig. 3.6 Variation of carrier mobility as a function of fast neutron fluence.

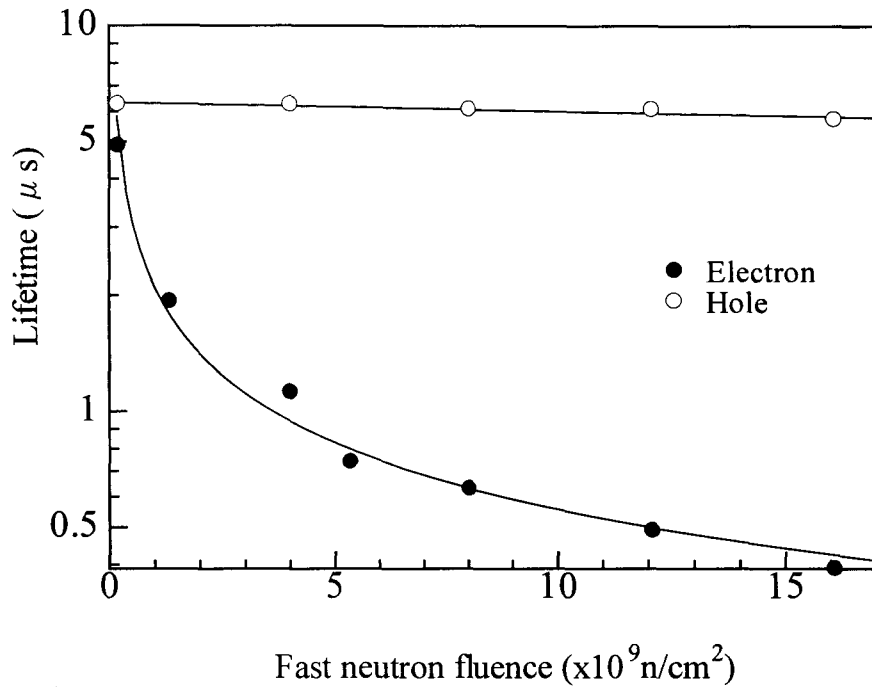


Fig. 3.7 Variation of carrier lifetime as a function of fast neutron fluence.

3.3.5 Comparison with Gamma-ray Irradiation

The effect of gamma-ray irradiation to the CdTe detector is well investigated by several authors. Taguchi et al.⁽⁷⁾ reported that the gamma-ray irradiation produces trapping centers of both signs. It is interesting that the gamma-ray irradiation seems to provide different influence on the performance of the CdTe detector. Therefore, the response characteristic of the gamma-ray heavily irradiated detector was examined using the two-dimensional spectrum analysis. The difference of the irradiation effect can be observed more apparently by comparing the results of both the experiments.

Figure 3.8 shows the two-dimensional spectrum of ¹³⁷Cs acquired from the gamma-ray heavily irradiated CdTe detector. With respect to the pulse amplitude, the position of the pulse distribution seems not to change. In contrast the distribution extends to much longer rise time. Moreover the pulse distribution newly appears in the region

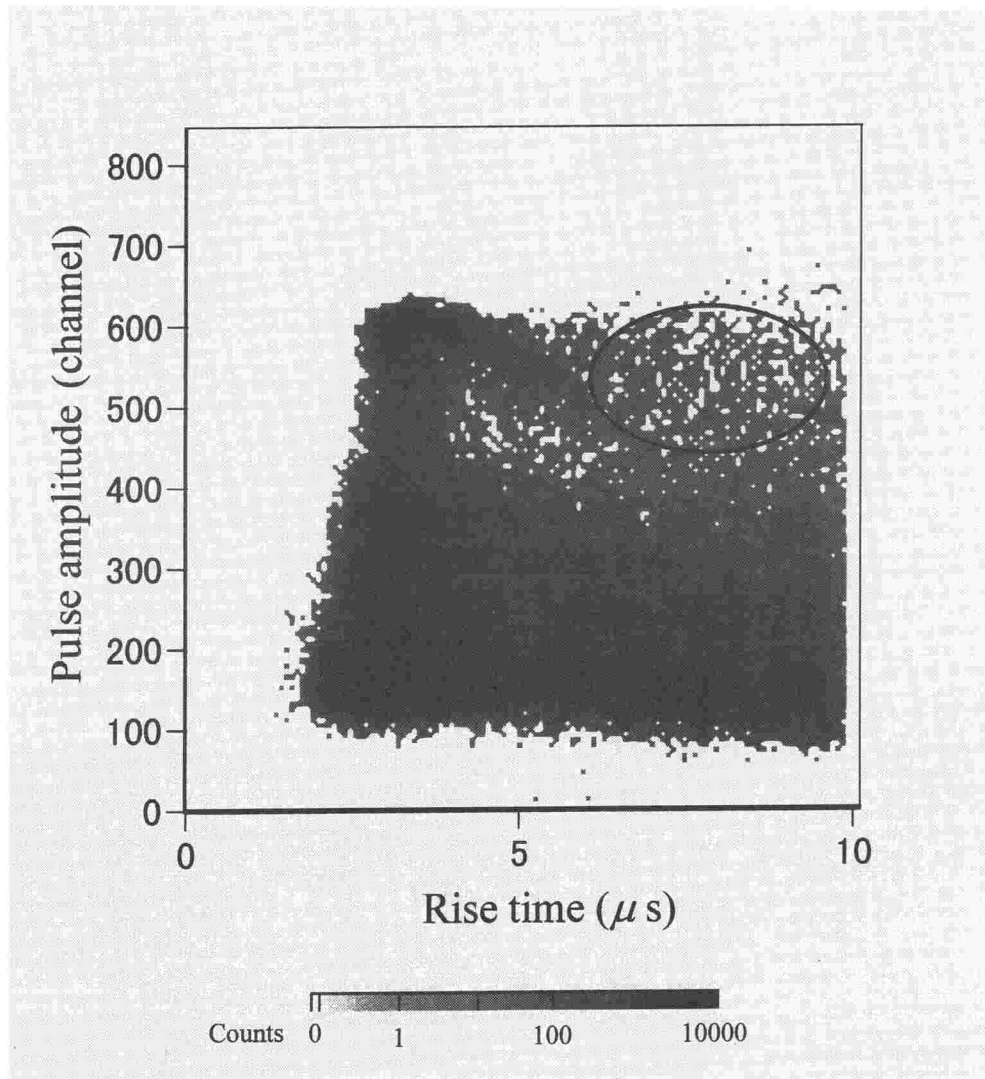


Fig. 3.8 Two-dimensional spectrum of ^{137}Cs measured with the gamma-ray heavily irradiated CdTe detector.

denoted as a circle in the figure. Cesium 137 spectra with different rise times are shown in Fig. 3.9. Comparing with the original spectrum as indicated in Fig. 3.4, the position of the main photopeak does not change for the spectra of 0-2 μ s. This result indicates that the effect of electron trapping is small in the case of the gamma-ray irradiation. On the contrary, the peak position changes to “higher” channels in the spectra over 3 μ sec. This peak shift can be seen clearly by comparing the peak positions in the spectrum of 4-5 μ sec for both Fig. 3.5(a) and Fig. 3.9. This peak corresponds to the cross-sectional view of the above mentioned new pulse distribution in the two-dimensional spectrum. Since the carrier trapping usually changes the peak position to “lower” channels, this result cannot be explained only by the carrier trapping. In addition to this, the broad photopeak is observed around 550 ch in the spectrum over 5 μ sec. This photopeak is likely to be composed by the longer rise time pulses with large pulse amplitude. When the holes are major for pulse formation, the generated pulse takes longer rise time, but the pulse amplitude becomes smaller due to the intrinsic trapping. Therefore, it can be concluded that the holes are not responsible for these broad photopeaks.

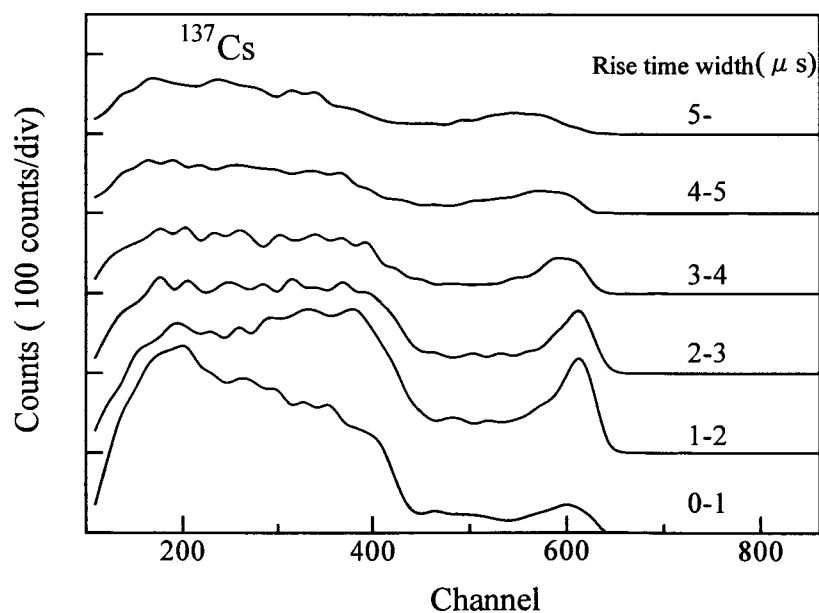


Fig. 3.9 ^{137}Cs spectra with different rise times acquired from the gamma-ray heavily irradiated CdTe detector.

Assuming that shallow electron-trapping centers are generated by the gamma-ray irradiation, the experimental result can be well explained. When part of the generated electrons are trapped by the centers during the transverse in the CdTe crystal and are detrapped after spending a few microseconds, these detrapped electrons contribute to pulse formation again with time delay. In this case the collection time of the electrons becomes longer, resulting in longer rise time. However the pulse amplitude does not change so significantly since the total charge collected to the electrode does not change. As a consequence, this pulse comes to have large amplitude and long rise time. The broad photopeak in the long rise time is composed by collecting such a pulse. It is probable that the electron detrapping is a characteristic feature of the gamma-ray irradiation effect.

Since the feature of the carrier detrapping is not observed from the two-dimensional spectrum acquired from the n-irradiated detector, it is appropriate to recognize that the effect of carrier detrapping is not appreciable for the fast neutron irradiation. Consequently, “deep” electron-trapping centers were generated by fast neutrons and as a result, they reduce the electron collection efficiency. The energy levels of intrinsic defects and/or impurities in CdTe have been studied and classified by other authors^{(10),(12)}. Figure 3.10 shows the common defect levels in a CdTe bandgap. It is well known that a cadmium (Cd) interstitial and a Cd vacancy give several trapping levels in correspondence with their charge states. A doubly charged Cd interstitial provides a deep trapping level of about 0.5 eV below the bottom of the conduction band (E_c)⁽¹³⁾. A shallow electron-trapping center ($E_c-0.02$ eV) is given by a Cd^+ interstitial. A doubly charged Cd vacancy gives about 0.7 eV below E_c and it plays as a recombination center⁽¹⁴⁾. As for radiation damage, an electron-trapping center (0.43 eV below E_c) has been observed in the CdTe irradiated with 2 MeV hydrogen ions⁽¹⁵⁾. Fast neutron irradiation probably generates a lot of defects with various types. However, shallow trapping centers might be annealed and recovered since the irradiation was conducted at room temperature. Other defects except the deep electron-trapping center are likely to give relatively small influence on the spectroscopic performance of the CdTe detector.

3.3.6 Annealing Experiment

Thermal behavior of the n-irradiated CdTe was examined with isochronal annealing.

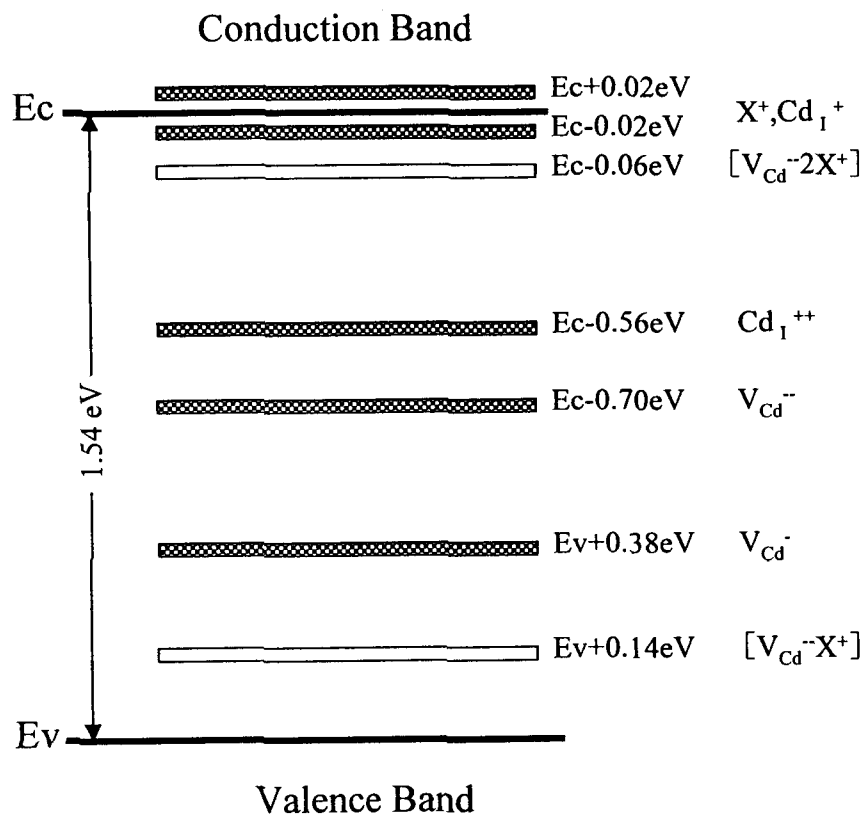


Fig. 3.10 Common defect levels in a CdTe bandgap (Ref. 10).

A CdTe specimen was irradiated with fast neutrons ($1 \times 10^{10} \text{ n/cm}^2$) before the annealing experiment. An infrared vacuum image furnace was used for heating from 50°C to 350°C with 50°C step. After completion of the heating, the specimen was taken from the furnace to fabricate the detector and after that, the pulse height spectrum of ^{137}Cs was measured at room temperature. The series of the spectra measured after heating is shown in Fig. 3.11. The spectra taken after the annealing of 100°C , 200°C , and 300°C are presented. The position of the 662 keV photopeak moves to the higher channels as the annealing temperature increases. This profile indicates that part of the electron-trapping centers are gradually recovered in accordance with the annealing temperature. The carrier collection loss becomes smaller, and hence the pulse amplitude becomes larger. The main photopeak does not change its position at 100°C , while it moves to the higher channels around 620 ch when the annealing temperature reaches 200°C . This peak shift corresponds to the increasing of the pulse amplitude of approximately 13 %. The detector performance was completely recovered after the annealing over 200°C .

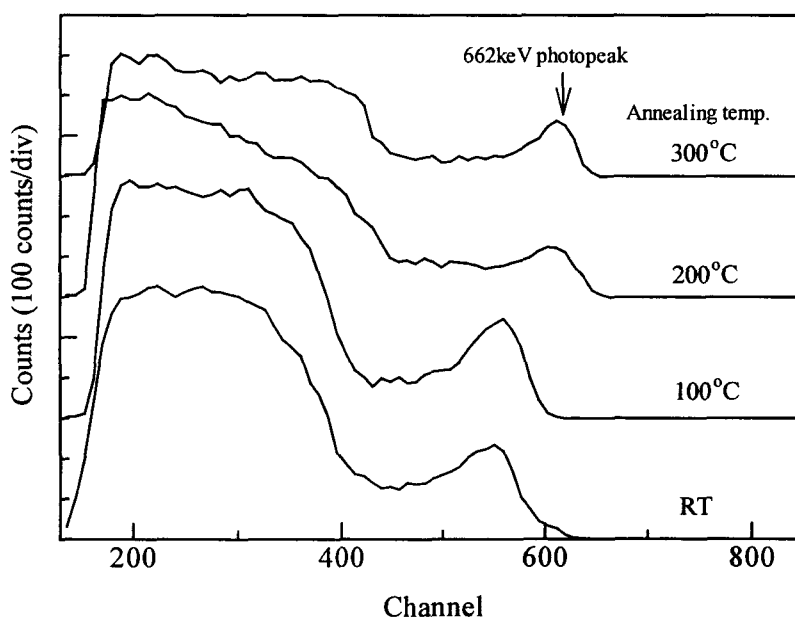


Fig. 3.11 ^{137}Cs gamma-ray spectra measured with the n-irradiated CdTe detector after annealing treatments.

Since the defect levels generated by fast neutrons have not been investigated for the CdTe detector, the assignment of the deep electron-trapping center is somewhat difficult. About the thermal behavior of the intrinsic defects in CdTe, it has been reported that the annealing with 140 °C causes the reduction of the deep trapping level of 0.37-0.55 eV band⁽¹⁶⁾. The annealing profile of the n-irradiated CdTe indicated that the temperature threshold of the defect recovery located around 150 °C. From this result, the thermal behavior of the electron-trapping center seems to be similar to that of the 0.37-0.55 eV band.

3.3.7 TSC Analysis

Thermally stimulated current (TSC) method is commonly used to characterize the defect levels in a semiconductor material⁽¹⁰⁾. In principle, the material is cooled to liquid nitrogen (L. N₂) temperature in a dark environment, and after that it is irradiated with laser, visible lights, or radiation. At that time carriers of both signs are generated and trapped at the several trapping centers in the material. As the temperature of the material increases, the trapped carriers which have enough energy are likely to be released from the center and they become a dark current. The increasing of the dark current is monitored as a function of the temperature. From the profile of the dark current, the energy level of the trapping center can be estimated.

In order to specify the deep electron-trapping center, the TSC measurement system was specially fabricated and was used for the n-irradiated CdTe. Schematic drawing of the TSC system is shown in Fig. 3.12. The CdTe specimen with electric contacts is set in a stainless vessel, and after that bias voltage of 50V is applied to the specimen from the outside of the vessel. The dark current is measured with a Pico-ammeter. Cool N₂ gas generated from liquid nitrogen is continuously introduced to the vessel to lower the temperature of the detector. After reaching minus 150 °C (123 K), dry argon gas is progressively fed into the vessel instead of the N₂ gas, so that the temperature of the specimen gradually increases with time. The temperature and the dark current of the specimen are simultaneously recorded with a digital pen-recorder.

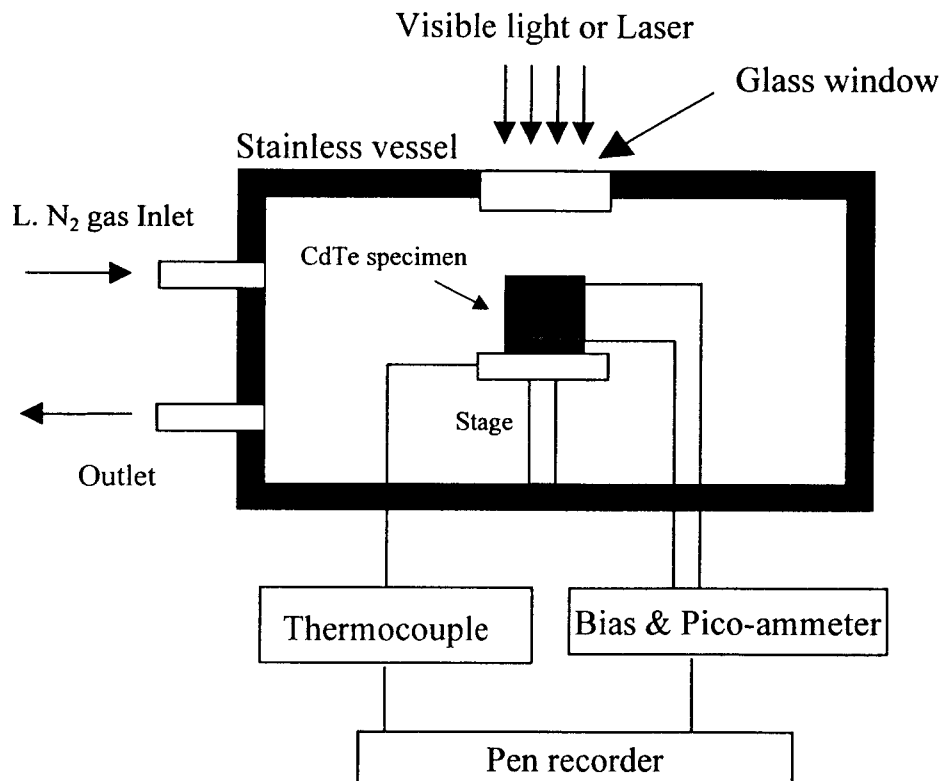


Fig. 3.12 Schematic drawing of the TSC measurement system.

Figure 3.13 compares the TSC spectra for the original and the n-irradiated CdTe. While any peaks cannot be observed for the original spectrum, the spectrum for the n-irradiated CdTe presents two distributions of the current peaks; one locates around 190 K and the other is 210~220 K. Since it seems that the concentration of the electron-trapping center is low, sufficient signal-to-noise ratio cannot be obtained in this study. However, assignment of these distributions were attempted by comparing the data of other reports^{(14),(17)}. The energy levels of the two distributions are assigned as; the temperature range of 185~195 K corresponds to the band energy of ~ 0.4 eV and the range of 200~220 K to ~ 0.5 eV. In the literature, the 0.4-0.6 eV band is related to the doubly-charged Cd vacancy or the Cd^{2+} interstitial^{(13),(14)}. The characteristics of the deep electron-trapping center are quite similar to that of these Cd-related centers. In addition, it is probable that Cd vacancies and interstitials are directly generated from the knock-on process by the fast neutrons and the following cascade. Consequently, it is appropriate to regard that lots of Cd^{2+} interstitials and the doubly-charged Cd vacancies are generated by fast neutrons and they construct deep trapping levels.

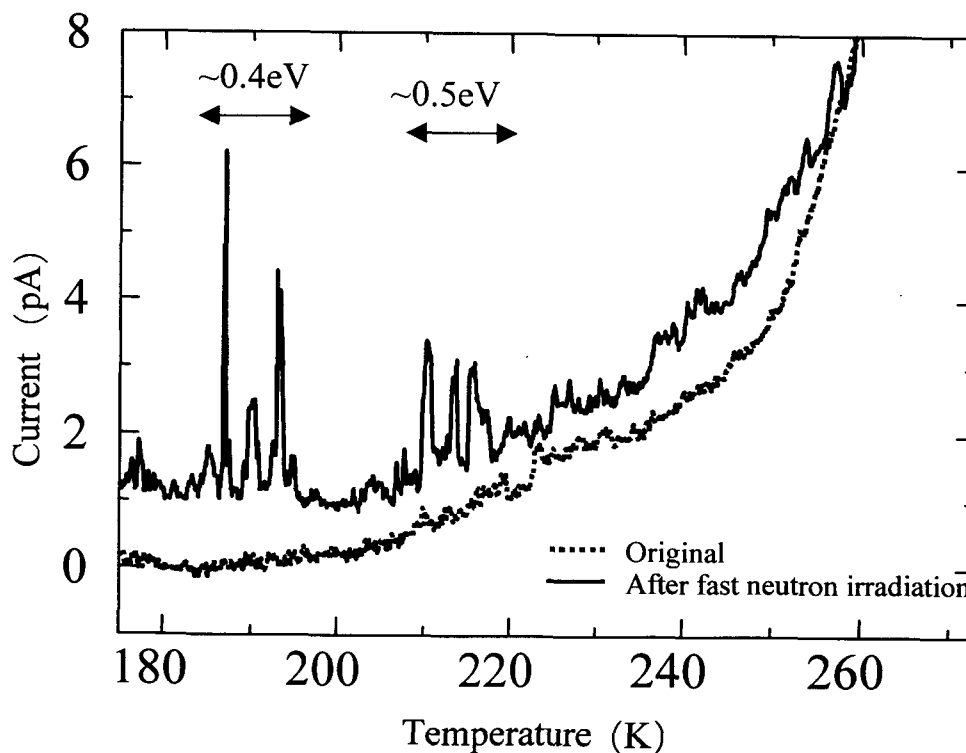


Fig. 3.13 TSC spectra for the original and the n-irradiated CdTe.

3.4 Conclusion

In this study, the degradation of detector performance was observed for the n-irradiated CdTe detector. The spectrum shape changed gradually with increasing the neutron fluence. Especially, the n-irradiated CdTe presented significant decreasing of the electron lifetime. Fast neutron irradiation was found to provide large influence on the electrons rather than the holes. The hardness of the CdTe detector against 14 MeV fast neutrons was experimentally examined; the detector kept its spectroscopic performance in the fluence below 1×10^{10} n/cm².

The difference of the irradiation effect between fast neutrons and gamma rays was clarified using the two-dimensional spectrum analysis. From the spectrum analysis, it was found that a deep electron-trapping center is generated by fast neutrons. The results of the annealing experiment and the TSC analysis supported that the deep electron-trapping centers were associated with the atom displacements by fast neutrons; the Cd vacancies and the interstitials.

References

1. H. Miyamaru, K. Fujii, T. Iida, and A. Takahashi, : J. Nucl. Sci. and Tech., Vol. 34, No.8, 755 (1997).
2. H. Miyamaru, K. Fujii, T. Iida, and A. Takahashi, : J. Nucl. Sci. and Tech., Vol. 33, No.9, 744 (1996).
3. H. Miyamaru, K. Fujii, T. Iida, and A. Takahashi, : *Ionizing radiation*, Vol.22, No.3 43 (1996).
4. Shoji, T. et al. : Nucl. Instr. Meth. Phys. Res., A322, 324 (1992).
5. Zanio, K. R. et al. : J. Appl. Phys., Vol39, No. 6, 2818 (1968).
6. Verger, L. et al., : Nucl. Instr. Meth. in Phys. Res., A322, 357 (1992).
7. Taguchi, T. et al., : Nucl. Instr. Meth., 150, 43 (1978).
8. Caillot, M. : Nucl. Instr. Meth., 150, 39 (1978).
9. Sumita, K. et al., : Nucl. Sci. Eng., 106, 249 (1990).
10. Schlesinger T. E. and James R. B., : "Semiconductors for Room Temperature Nuclear Detector Applications", Academic Press, Vol. 43 (1995).

11. Manfredotti, C. et al., : Nucl. Instr. Meth. Phys. Res., A322, 331 (1992).
12. Hoschl, P. et al., : Nucl. Instr. Meth. Phys. Res., A322, 371 (1992).
13. Hage-Ali, M. and Siffert, P. : Nucl. Instr. Meth. Phys. Res., A322, 313 (1992).
14. Huang, Z. C. et al., : Nucl. Instr. Meth. Phys. Res., B100, 507 (1995).
15. Mergui, S. et al., : Nucl. Instr. Meth. Phys. Res., A322, 381 (1992).
16. Mergui, S. et al., : Nucl. Instr. Meth. Phys. Res., A322, 375 (1992).
17. Biglari, B. et al., : J. Appl. Phys., 65, (3), 1112 (1989).

Chapter 4

Effects of Deuterium Ion Implantation on Carrier Transport

Property of CdTe Detectors

The influence of deuterium (D) ion implantation to the CdTe detector was studied⁽¹⁾. Variation of carrier mobility was evaluated as a function of D ion fluence. The 5.5 MeV α particle from a ^{241}Am source was measured with the ion-implanted detector to evaluate the mobility for individual carrier. Two-dimensional spectrum of the α particles was also acquired with the RTD processing. The electron mobility increased at lower fluence range, while the mobility for both carriers markedly decreased over the fluence of 1×10^{13} ions/cm². Experimental results indicated that the passivation of the intrinsic defects was caused by the implanted D atoms.

4.1 Introduction

From earlier stage of the development, material characteristics of CdTe have been well studied ⁽²⁾⁻⁽⁴⁾. The role of intrinsic defects in CdTe has been clarified, in which they influenced seriously on the carrier transport property of the detector ⁽⁵⁾. In addition, these defects were found to cause several difficulties such as polarization effect ⁽³⁾ and carrier collection loss ⁽⁴⁾. For the performance enhancement, one of the important techniques is defect compensation by the addition of some specific elements ^{(6),(7)}. Especially, the behavior of hydrogen (H) in CdTe has been recently focused and reported in several papers ⁽⁸⁾⁻⁽¹⁰⁾. Hydrogen introduced by diffusion or ion implantation played as a defect compensator ⁽⁹⁾. Furthermore it has been reported that passivation of the intrinsic defects leads to the improvement of electrical property for the H implanted CdTe ⁽¹⁰⁾. Although the detector performance strongly depends on the carrier transport property, the influence of hydrogen or its isotopes to this property has not been experimentally examined. This chapter describes the influence of D ion implantation to the CdTe detector. Variation of carrier mobility is evaluated as a function of D ion fluence. The relationship is discussed between the carrier transport property of the implanted detector and the concentration of the implanted D atoms.

4.2 Experimental Setup

The p-type CdTe radiation detector (CDTE2BE, Toyo Medic Co.) was prepared for ion implantation. The implantation was carried out with the deuteron accelerator OKTAVIAN ⁽¹¹⁾ at room temperature. Experimental setup is illustrated in Fig. 4.1. A vacuum chamber built in the accelerator is evacuated to keep pressure of approximately 10^{-4} Pa during the implantation. The detector is fixed at the center of the chamber and an aluminum plate with an aperture (2 mm in diameter) is attached in front of the detector for beam collimation. After passing through the aperture, deuterium ions with an energy of 250 keV are injected to the CdTe crystal through a negative electrode side. During the implantation, the beam current was kept to be approximately 4 nA to reduce temperature rise of the detector. The implantation was conducted with the fluence ranging from 2.4×10^{12} to 5.2×10^{15} ions/cm². The carrier mobility was examined at

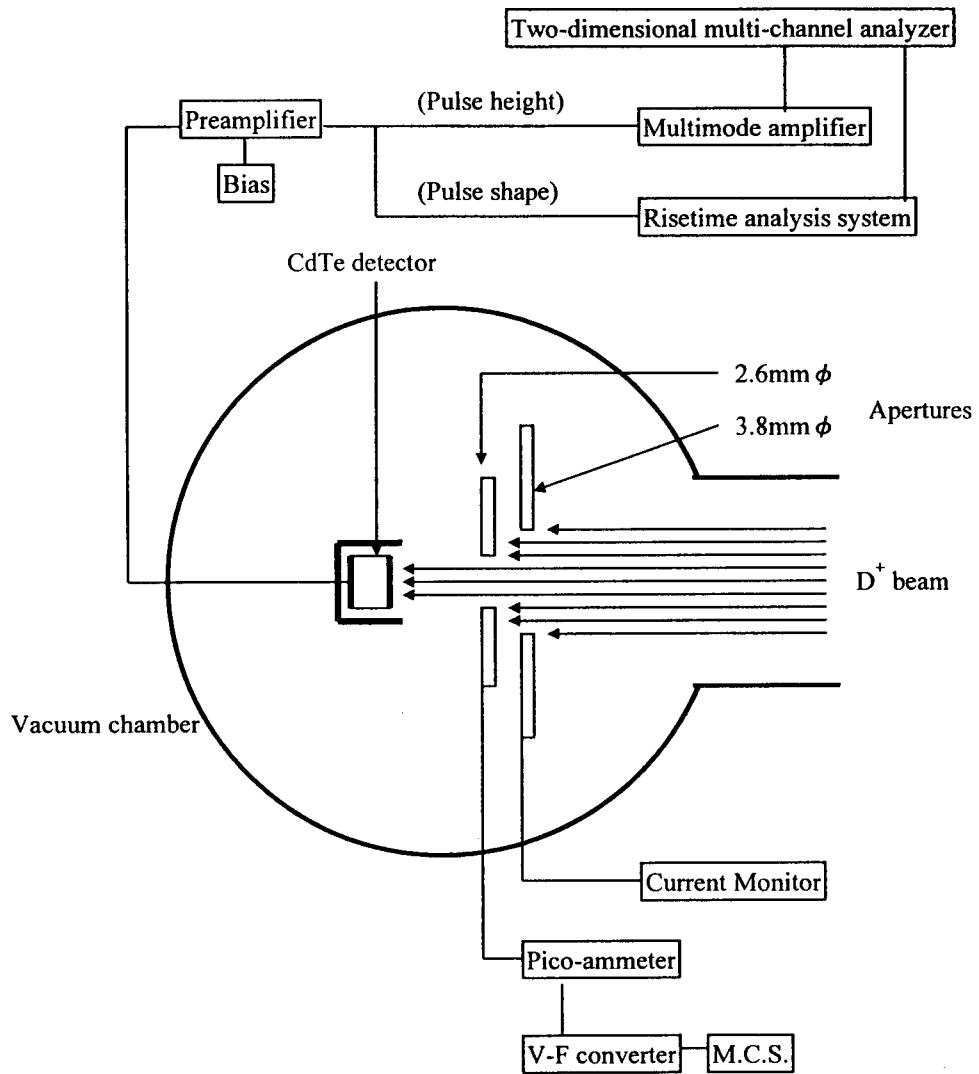


Fig. 4.1 Experimental setup for D ion implantation.

several stages in the fluence range.

Since the rise time fluctuation of a response pulse occurs when measuring a high-energy gamma-ray, it is somewhat difficult to obtain the accurate value of the carrier mobility from the pulse shape. Therefore 5.5 MeV α particles from an ^{241}Am source was measured instead of gamma-rays. The α particle deposits its energy in quite short distance from the surface of the injected electrode side because of the large energy loss. At that time, generated carriers initially concentrate near the injected electrode side, and then this allows one carrier species to move along the detector thickness to the other electrode. Thus the transit time of the specific carrier can be evaluated from the pulse rise time. The carrier mobility is calculated from the experimental data of the transit time, the detector thickness and the bias voltage. Each carrier is collected individually by applying inverted bias polarity. To measure the rise time, every pulse shape was directly recorded and stored with a fast digital oscilloscope (LeCroy 9384). The rise time fluctuation of the stored pulses was evaluated and the average of the rise time was used to determine the carrier mobility. The system for measuring the pulse height spectrum consisted of a pre-amplifier (CLEAR PULSE 656), a spectroscopy amplifier (ORTEC 543), and a multi-channel analyzer (ORTEC 7800). In addition, the two-dimensional spectrum of the α particle was obtained from the RTD processing system which is described in Chapter 2. The effect of deuterium ion implantation is examined from the two-dimensional spectrum.

4.3 Deuterium Ion Implantation

4.3.1 Measurement of 5.5 MeV α Particles

The diffusion profile of the implanted D atoms depends on their concentration and the temperature of the bulk CdTe. It is likely that the concentration gradually varies from the irradiated front side to the back side just after finishing the implantation. This concentration gradient seems to cause performance instability of the implanted detector. Actually, we observed that the full energy peak of the α particle gradually shifted during the measurement time. In our experimental condition, the position of the peak was finally fixed and remained unchanged after spending enough time, approximately ten

hours after finishing the irradiation. Therefore the transient peak shift seems to appear during the time period in which the diffusion of the D atoms proceeds in the bulk. However, this "diffusion effect" is not discussed here. After spending much time from the implantation, the detector provided stable spectroscopic performance. Figure 4.2 shows a stacked plot of the α particle spectrum with different D ion fluence. Each spectrum was acquired with the implanted detector after spending a long time period (approximately twelve hours) from the implantation. The α particles were injected from the negative contact side. It is probable that the radiation damage by the ion implantation may affect the detector performance. However, the distance accompanied with the radiation damage by the implantation is quite short (a few micrometer) comparing with the total drift length of the carriers generated by the α particles. Thus the influence of the radiation damage is negligible and accordingly, variation of the spectrum shape originates from the change of the carrier transport property by the implanted D atoms. At the initial implantation stage, the position of 5.5 MeV peak slightly shifts to higher channels and it locates approximately 5 % higher energy than that for before implantation. This is an important feature of the D ion implantation effect. Figure 4.2(b) shows the spectra in the higher fluence range. It is shown that the peak position markedly shifts to the lower energy side with increasing the fluence. The FWHM of the peak becomes broader and the increasing of electrical noise is also observed at the higher fluence. When the detector was implanted with the fluence over 1.5×10^{15} ions/cm², the peak position could not be identified due to the significant increasing of the noise.

Two-dimensional spectra of the 5.5 MeV α -particle are presented in Figs. 4.3 and 4.4. Also in this measurement, the α -particles were injected to the detector from the negative contact side, and then the electrons are major for spectrum formation. The horizontal axis corresponds to the pulse rise time and the pulse amplitude to the vertical axis. The contour of the pulse distribution corresponds to the difference of the pulse count. Before implantation, the response profile of the α particle shows point-like distribution which concentrates at the shorter rise time of 0.4 μ s. The distribution, firstly, expands to lower amplitude side with increasing the fluence as indicated in Fig. 4.3. Since the α -particle deposits its energy in the region accompanied with the defects caused by the implantation, a part of the generated carriers seems to be trapped by the defects and does not take part in pulse formation. This trapping effect may cause peak tailing to

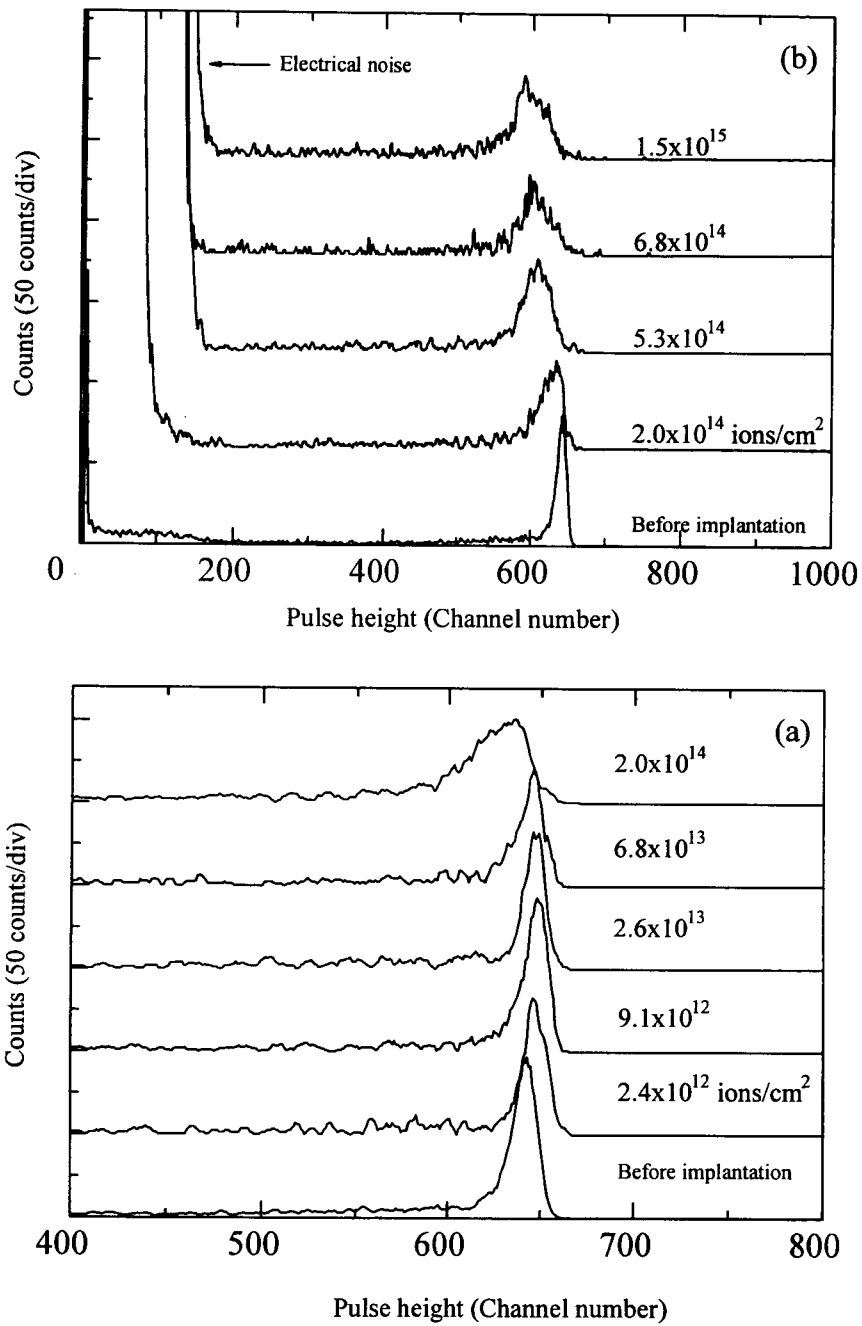


Fig. 4.2 Stacked plot of 5.5 MeV α particle spectra measured with the CdTe detector implanted with D ions in (a) lower and (b) higher fluence range.

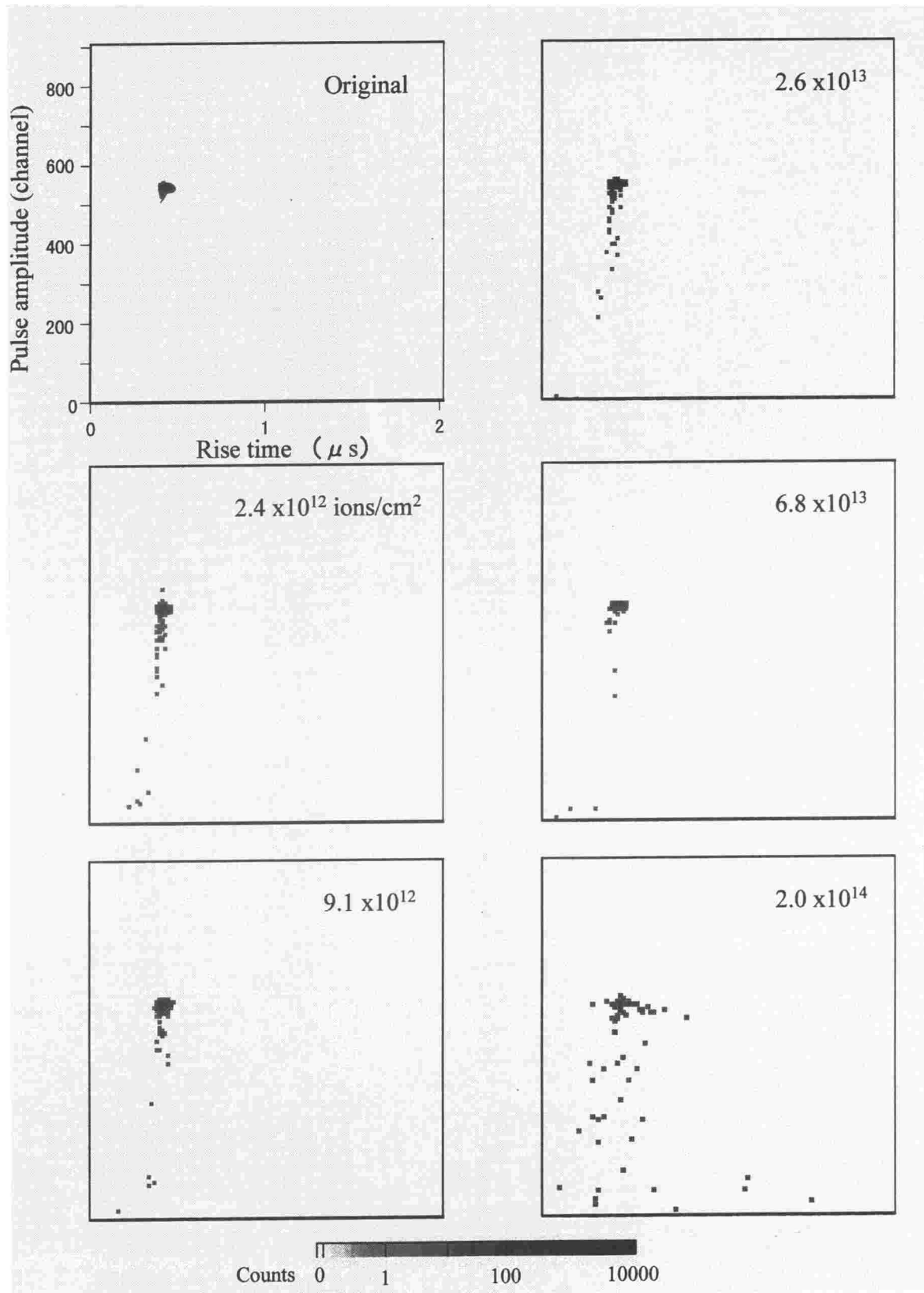


Fig. 4.3 Two-dimensional spectra of the α particle in the D ion fluence range below 2.0×10^{14} ions/cm².

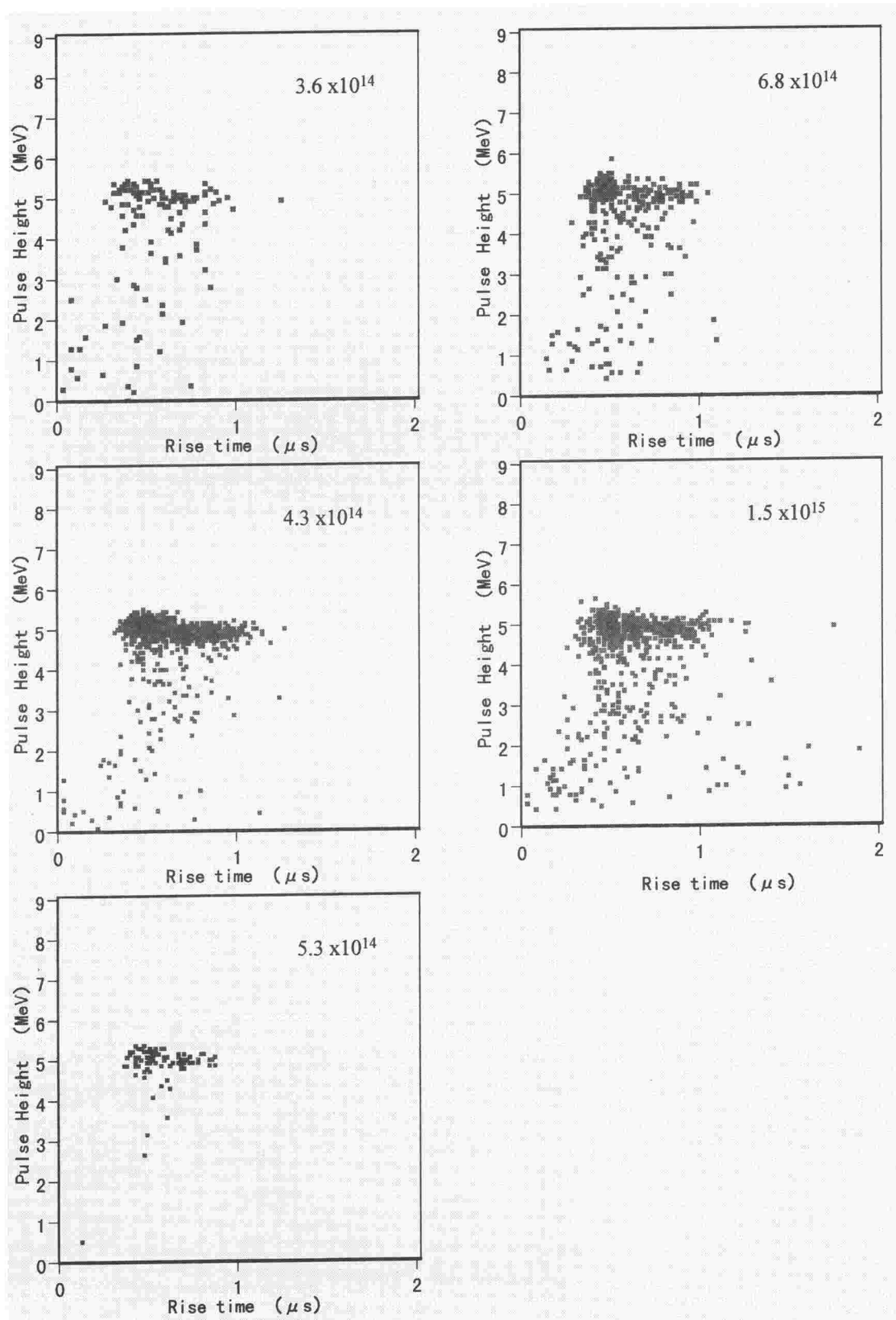


Fig. 4.4 Two-dimensional spectra of the α particle in the higher fluence range 3.6×10^{14} - 1.5×10^{15} ions/cm².

the lower side. When proceeding the implantation, the distribution markedly expands to the rise time axis as typically shown in Fig. 4.4. Since the longer rise time pulse originates from the longer collection time of the electrons, this result indicates that the electron mobility gradually decreases with increasing the ion fluence.

4.3.2 Spectroscopic Performance

Figure 4.5 shows the ^{241}Am gamma-ray spectra measured with the original (a) and the detector implanted with 1.5×10^{15} ions/cm² (b), respectively. The detectors were exposed to the gamma rays from the negative contact side. The position of the 59.5 keV photopeak shifts to lower channels (80 % of the original) and the FWHM of the peak changes from 3 keV to approximately 20 keV. The detector performance is apparently degraded by the excessive implantation.

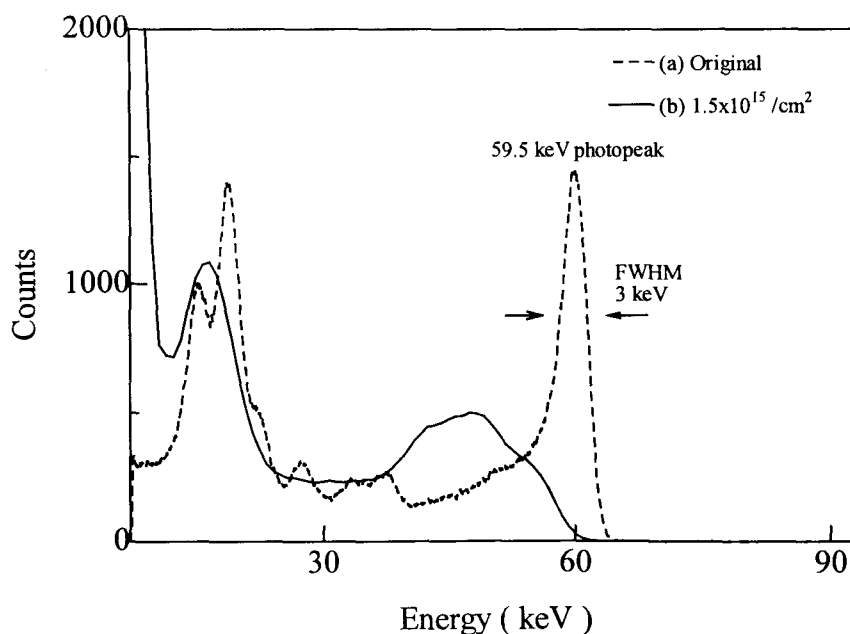


Fig. 4.5 ^{241}Am gamma-ray spectra measured with the CdTe detectors.
(a) Original, (b) After the ion implantation with 1.5×10^{15} ions/cm².

4.3.3 Carrier Mobility

Figure 4.6 shows the carrier mobility for respective electrons and holes as a function of the D ion fluence. The error level of the carrier mobility corresponds to the rise time fluctuation of the measured pulses. The electron mobility gradually increases with increasing the fluence at lower fluence, however it decreases significantly after the prolonged implantation. The maximum of the electron mobility shows 5 % increase at the fluence of 9.1×10^{12} ions/cm². On the contrary, the hole mobility decreases monotonously with the fluence. It was found that the hole mobility did not increase in any fluence range of this study.

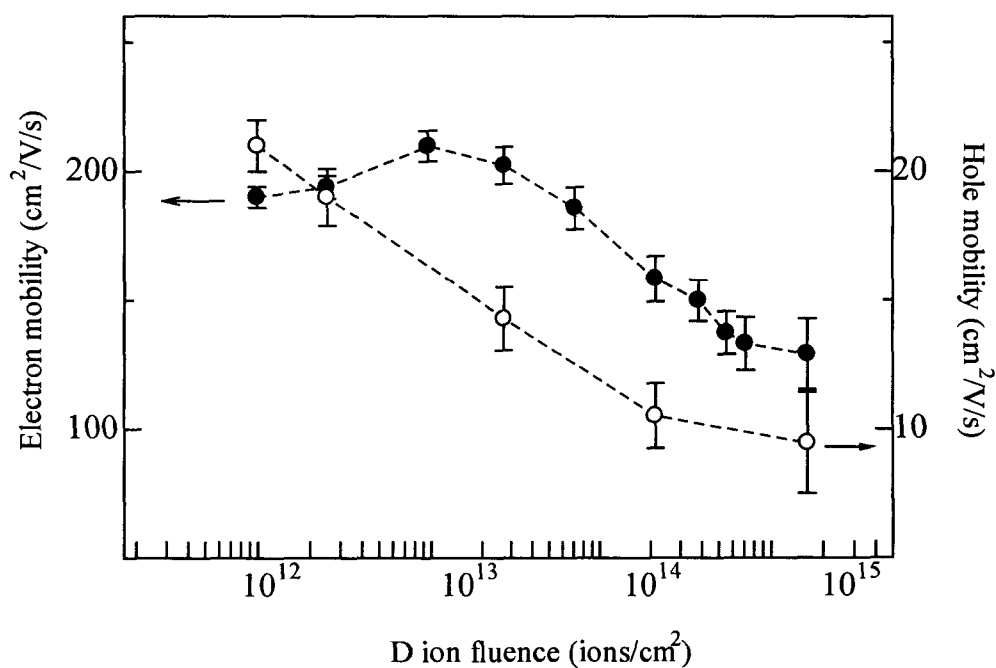


Fig. 4.6 The change of carrier mobility as a function of D ion fluence.

4.3.4 Polarization Effect

Polarization effect is characterized as any change in the spectroscopic performance of the detector over time. Historically, the polarization effect was a serious problem for the CdTe detector⁽¹²⁾. However the recent development of the crystal growth technique enables one to produce the CdTe crystal with high quality, and then the polarization effect by intrinsic defects provides much smaller influence for the latest CdTe detectors. However, it has been clarified that the CdTe and/or HgI detectors irradiated with gamma-rays presented the polarization effect⁽¹³⁾. Also in this study, the polarization effect was observed for the CdTe detector implanted with D ions. Figure 4.7 shows the pulse amplitude of the 59.5keV gamma ray versus operation time. The amplitude is normalized by the one measured just after applying the bias. The amplitude decreases gradually with the operation time and becomes approximately 90 % of the original after 200 min. Since this change exceeds ordinary fluctuation ($\sim 2\%$), it seems that the implanted D ions construct space-charge layer in the CdTe and decrease the amplitude of the “effective” electric field.

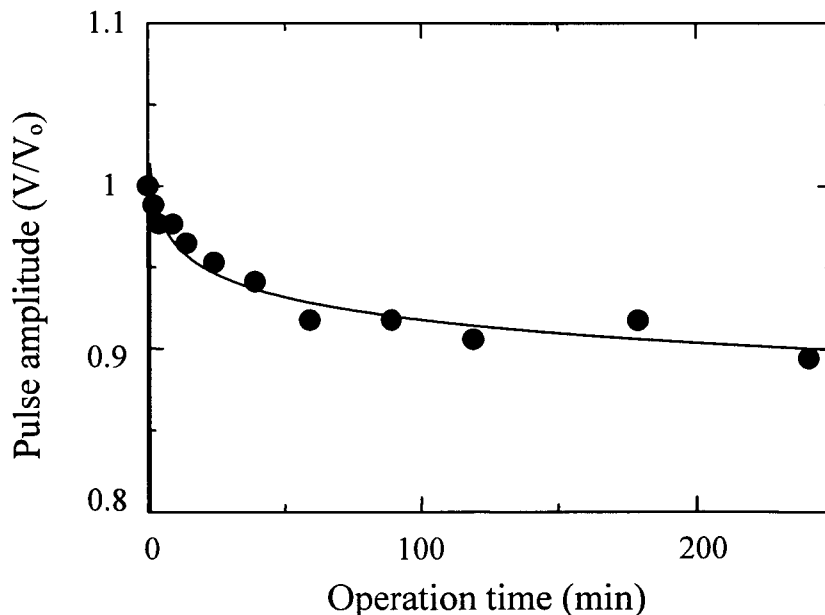


Fig. 4.7 Variation of the pulse amplitude versus operation time.

4.4 Conclusion

Our experimental results presented good agreement with the reported passivation effect for the transport property of electrons⁽¹⁰⁾. The increasing of the electron mobility at the lower fluence can be interpreted due to the passivation of the intrinsic defects by the D atoms. The higher electron mobility enhances carrier collection efficiency of the detector, and as a result the peak shift to the higher channels occurs. In contrast, the hole mobility did not improve at any fluence range examined in this study. The important point is that the passivation by the D atoms becomes effective only for the electron. It was also indicated that excessive implantation leads to the significant decreasing of the carrier mobility for both carriers. From the experimental results, the carrier mobility was found to change with the concentration of the implanted D atoms. Although the detailed mechanism of the passivation is not clear, our results suggest the fact that the quantitative ratio between the implanted D atoms and the intrinsic defects is a key factor to characterize the electron transport property.

References

1. H. Miyamaru, K. Fujii, A. Takahashi, : J. Nucl. Sci. and Tech., Vol. 35, No.9, 679 (1998).
2. Zanio, K. R., et al.: J. Appl. Phys., Vol.39, No 6, 2818 (1968).
3. Siffert, P., et al.: IEEE Trans., Nucl. Sci., NS-23, 1, 159 (1976).
4. Siffert, P.: Nucl. Instrum. Methods, 150, 1 (1978).
5. Schlesinger, T. E. and James, R. B.: "Semiconductors for Room Temperature Nuclear Detector Applications", Academic Press, Vol. 43, New York, (1995).
6. Ohmori, M. and Iwase, Y.: Mater. Sci. and Eng., B16, 283 (1993).
7. Shoji, T., et al.: IEEE Trans., Nucl. Sci., Vol. 40, No.4, 405 (1993).
8. Hage-Ali, M., Siffert, P.: Nucl. Instrum. Methods, Phys. Res., A322, 313 (1992).
9. Mergui, S., et al.: Nucl. Instrum. Methods, A 322, 381 (1992).
10. Biglari, B., et. al.: J. Appl. Phys., 65, 3, 1112 (1989).
11. Sumita, K., et al.: Nucl. Sci. Eng., 106, 249 (1990).
12. Akutagawa, W. and Zanio, K.: J. Appl. Phys., Vol.40, No 9, 3838 (1969).

13. Gerrish, V.: Nucl. Instrum. Methods, Phys. Res., A322, 402 (1992).

Chapter 5

Improvement of Radiation Response Characteristic on CdTe Detectors using Fast Neutron Irradiation

The treatment of fast neutron pre-irradiation was applied to a CdTe detector in order to change the response characteristic⁽¹⁾. The pre-irradiation treatment was aimed to improve energy resolution for high-energy gamma rays. Spectroscopic performance of the pre-irradiated detector was compared with the original. Additionally, the detector was employed with the processing of rise time discrimination (RTD). Pulse height spectra of ^{241}Am , ^{133}Ba , and ^{137}Cs gamma rays were measured to examine the change of the detector performance. Electron lifetime decreased by the irradiation and this change provided the detector with different response characteristic. The pre-irradiated CdTe detector presented better energy resolution for higher-energy photons comparing with the original. The combination of the pre-irradiated detector and the RTD processing was found to provide further enhancement of the energy resolution. Application of fast neutron irradiation effect to the CdTe detector was demonstrated.

5.1 Introduction

In recent years, cadmium telluride (CdTe) radiation detectors have been widely used for the measurement of low-energy photons and their application also spreads over various fields such as nuclear medical diagnostics ^{(2), (3)}, undestructive monitor ⁽⁴⁾ and astrophysical research ⁽⁵⁾. While the detector provides better energy resolution for lower-energy photons, the resolution is not enough especially for high-energy photons above 100 keV. Now a day, further development is expected for broader application. Several techniques have been proposed to develop the performance of the CdTe detector ⁽⁶⁾⁻⁽⁸⁾. The resolution enhancement has been successfully accomplished by cooling the detector or by applying high bias voltage ^{(6),(9)}. In these cases, performance enhancement is obtained by improving the carrier transport property of the detector. This property depends on not only operating temperature or bias voltage but also the nature of CdTe material itself ⁽¹⁰⁾⁻⁽¹²⁾. In this chapter, application of the fast neutron irradiation effect to the CdTe detector is described. The pre-irradiation with 14 MeV fast neutrons was carried out to improve the performance of the planar-type CdTe detector. The spectroscopic performance of the pre-irradiated CdTe detector was compared with the original to evaluate the pre-irradiation effect. Additionally, the detector was employed with the RTD processing. The effectiveness of the pre-irradiation treatment is discussed.

5.2 Principle

The planar-type CdTe detector is generally subjected with radiation through a negative contact side. When the energy of incident radiation is low, most electron-hole pairs are generated near the negative side because of large attenuation of CdTe⁽¹⁹⁾. In this case the electrons contribute pulse formation rather than the holes since the holes are collected quickly to the negative contact. Because of large mobility of the electrons, the generated electrons are effectively collected and then charge collection loss can be reduced. Hence the detector provides good energy resolution for lower energies. When radiation interaction positions extend uniformly to the whole sensitive volume of the detector, as is the case for high-energy photons, both carriers take part in

pulse formation almost equally. At this time the charge collection loss becomes remarkable due to smaller mobility of the holes. Since the degree of the collection loss depends on hole drift length, the difference of the interaction position causes the fluctuation of pulse amplitude. This amplitude fluctuation degrades the energy resolution for higher-energy photons.

For the radiation response of the planar-type CdTe detector, the pulse amplitude can be briefly expressed as a function of pulse rise time (T)^{(4),(7),(20)},

$$V(T) = \frac{Q_o \cdot E}{C \cdot d} \left[\mu_e \tau_e \left\{ 1 - \exp\left(-\frac{T}{\tau_e}\right) \right\} + \mu_h \tau_h \left\{ 1 - \exp\left(-\frac{T}{\tau_h}\right) \right\} \right] \quad (1)$$

where Q_o : Total charge generated by radiation
 E : Amplitude of applied electric field
 C : Device capacitance
 d : The distance between two electrodes
 μ_e, μ_h : Carrier mobility for electrons and holes
 τ_e, τ_h : Lifetime for individual carrier.

The collection time of each carrier depends on the radiation interaction position (x : the distance from the negative electrode) as

$$T_e = \frac{d-x}{\mu_e E} \quad \text{and} \quad T_h = \frac{x}{\mu_h E}.$$

The rise time is specified by the longer collection time either T_e or T_h . For simplicity, uniform electric field and single trapping for each type of the carrier are considered in this formula. In order to examine the profile of pulse amplitude fluctuation in rise time, brief calculation was carried out with Eq. 1. The dimensions of the detector and several parameters used are summarized in Table 5.1. Generally,

the electron mobility is approximately 10 times larger than that of a hole and both lifetimes are almost the same as a few microseconds for the CdTe detector ⁽²⁰⁾⁻⁽²²⁾. Therefore the values of 500 and 50 cm²/Vs were assumed for μ_e and μ_h respectively. When mono-energetic photons interact at random positions in the sensitive volume of this detector, the relation between the pulse amplitude and the rise time can be expressed as a solid line in Fig. 5.1. This is somewhat rough approximation of real response, but the rise time dependency of the pulse amplitude can be estimated. The time constant of the pulse shaping is assumed to be longer enough than the collection time. As indicated in the figure, the pulse amplitude presents monotonous (but not linear) decreasing with increasing the rise time. This profile represents the response characteristic of the CdTe detector for high-energy photons. Considering the detector thickness of conventional planar-type CdTe detectors, it is likely that most of them take the order of a few millimeter. In this thickness range, the response characteristic of the real detector shows good agreement with the profile of our simulation. Since the projection of this profile toward the pulse amplitude axis corresponds to the peak width of a full-energy peak, this amplitude fluctuation results in peak tailing to lower energy side. Consequently, the amplitude fluctuation is attributed to the large difference of the transport property between electrons and holes and it degrades the energy resolution for high-energy photons.

Table 5.1 Several parameters employed in the calculation.

Parameter	Value
d (mm)	1
E (V/cm)	500
μ_e (cm ² /Vs)	500
μ_h (cm ² /Vs)	50
τ_e (μ s)	0.6-12
τ_h (μ s)	6

Basic idea for the resolution enhancement is to improve the response characteristic by using the effect of fast neutron irradiation. As described in the previous chapter, the electron transport property significantly changes by the effect of fast neutron irradiation.

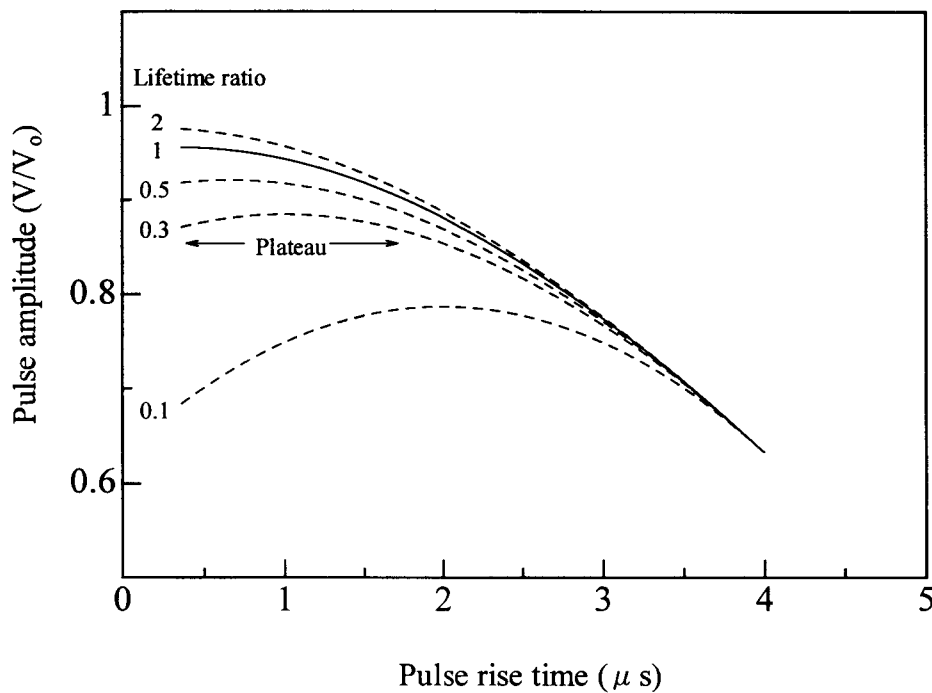


Fig. 5.1 The relation between pulse amplitude and rise time on the response of the planar-type CdTe detector. Pulse amplitude is normalized by the one of full collection ($V_o=Q_o/C$).

This irradiation effect was employed to change the response characteristic of the CdTe detector. Figure 5.2 shows the carrier lifetimes as a function of fast neutron fluence. The electron lifetime decreases markedly by the irradiation, in contrast the one for holes does not show meaningful change. Accordingly, the ratio of the lifetimes (τ_e/τ_h) takes a different value after irradiating. This change of the lifetime ratio provides the CdTe detector with different response characteristic. The response function with different lifetime ratio was calculated and the resulting curve is shown as broken lines in Fig. 5.1. The functions with the ratio of 2, 1, 0.5, 0.3 and 0.1 are presented respectively. These conditions can be realized by the irradiation with the fluence range $1-5 \times 10^9$ n/cm². As far as low fluence irradiation below 1×10^{10} n/cm² is concerned, the change of the carrier mobility is confirmed to be less than 10%. Therefore the collection times (T_e and T_h)

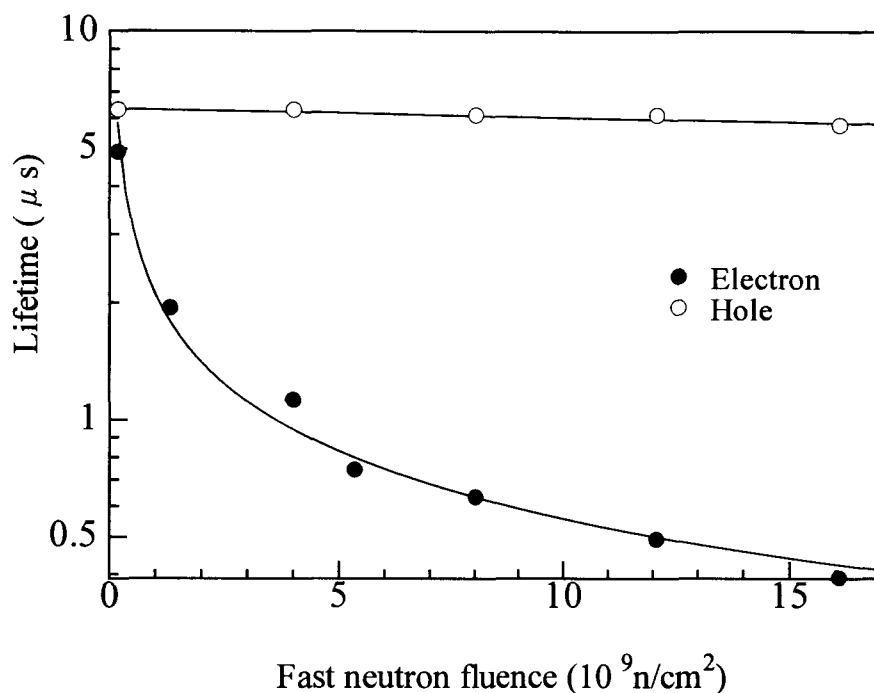


Fig. 5.2 The variation of carrier lifetime of the planar-type CdTe detector as a function of fast neutron fluence.

can be assumed not to change so significantly by the pre-irradiation treatment. For this reason, the change of the rise time range is not taken into account in this simulation. Since the shorter lifetime increases the probability of carrier trapping, the contribution of the generated electrons to the pulse formation becomes smaller when the electron lifetime decreases. Therefore, the pulse amplitude at the short rise time decreases gradually with decreasing the lifetime ratio. It is important to note that the function at the ratio of 0.3 becomes rather drawing plateau than the original ($\tau_e/\tau_h = 1$). This simulation suggests that the optimized lifetime ratio suppresses the amplitude fluctuation in the short rise time. In general, the number of the pulse at the shorter rise time becomes relatively larger than that for longer rise time on the measurement of high-energy photons ^{(6), (7)}(see Fig. 2.8 in Chapter 2). Thus the amplitude fluctuation in the short rise time gives large contribution to the spectrum shape. From this point,

the plateau response function is effective against the resolution enhancement. Table 5.2 summarizes the calculated value of the amplitude fluctuation at the different lifetime ratio. The fluctuation width was acquired as a difference between the minimum and the maximum of the pulse amplitude in the rise time range below 2 μs . The amplitude fluctuation decreases with decreasing the lifetime ratio. The fluctuation in the short rise time is markedly suppressed at the ratio of 0.3 in this simulation. However, excessive decreasing of the lifetime ratio causes large fluctuation oppositely. The optimized response function can be specified by changing the lifetime ratio. When the pre-irradiated detector is used with the RTD processing, only the shorter rise time pulses can be collected selectively to form the pulse height spectrum. Therefore the pre-irradiation treatment presents its effectiveness more clearly when the detector is used with the RTD processing.

The response characteristic is determined not only by the carrier transport property but also by the size of the CdTe detector and the operating condition. From the practical view, the optimized response characteristic is determined individually for each CdTe detector. The pre-irradiation effect is demonstrated experimentally by using a commercial CdTe detector.

Table 5.2 The pulse amplitude fluctuation in rise time.

Lifetime Ratio (τ_e/τ_h)	Pulse Amplitude Fluctuation (%)
2	8.7
1	7.5
0.5	5.3
0.3	3.7
0.1	10.7

5.3 Experimental Procedure

The planar-type CdTe radiation detector (CDTE2BE) was prepared for fast neutron pre-irradiation. This detector is well introduced in Chapter 1. The detector was

housed in an aluminum chamber with a beryllium window attached to the front side of the chamber. Two CdTe detectors that have almost the same spectroscopic performance were used; one was pre-irradiated with 14 MeV fast neutrons and the other was used for reference. Neutron fluence for the pre-irradiation was approximately 1.0×10^9 n/cm². The pre-irradiation was conducted with the deuteron accelerator OKTAVIAN⁽²³⁾ at room temperature.

In order to observe the pre-irradiation effect clearly, two types of measurement systems were prepared; one was a conventional setup for the spectroscopy; a pre-amplifier (CLEAR PULSE 656), a spectroscopy amplifier (ORTEC 672) and a multi-channel analyzer (ORTEC 7800) and the other was a system with the RTD processing. The principle of the RTD processing is described in Chapter 2, so that the explanation of this system is not described here. The detector performance was evaluated by measuring gamma rays of ²⁴¹Am, ¹³³Ba and ¹³⁷Cs from radioactive source respectively. The detector was operated with the voltage of 50V (625 V/cm) throughout our study and all measurements were conducted at room temperature. The pulse shaping of the multimode amplifier was set to be 2 μ s. A precision time calibrator (ORTEC 462) was used to calibrate the pulse rise time.

5. 4 Results and Discussions

5. 4. 1 Detector Characteristics

Radiation damage becomes a main cause of the leakage current increasing for semiconductor-type radiation detectors ⁽⁶⁾. For the CdTe detector, large leakage current increases detector noise and degrades energy resolution ⁽¹⁹⁾. It seems probable that fast neutron pre-irradiation also causes such difficulties. Firstly, we examined the electrical characteristic of the pre-irradiated CdTe detector. Current-voltage characteristics are plotted in Fig. 5.3 for the original and the pre-irradiated detector. The characteristic of a heavily pre-irradiated detector is also indicated. Comparing with the characteristic of the original, remarkable change is not observed for the pre-irradiated detector, while the heavily pre-irradiated one presents large increasing of the leakage current. This result indicates that the leakage current increasing by the pre-irradiation can be negligible as

far as the neutron fluence is low.

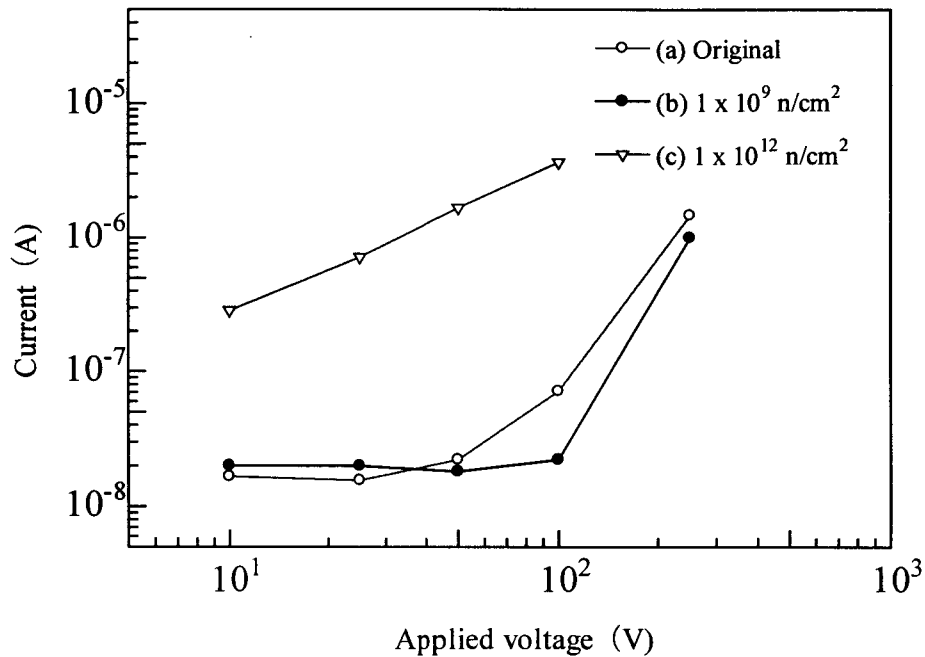


Fig. 5.3 Current-voltage characteristics of the CdTe detectors. The characteristics of three detectors are compared; (a) original, (b) pre-irradiated with 14 MeV fast neutrons (1.0×10^9 n/cm²) and (c) heavily pre-irradiated (1.0×10^{12} n/cm²).

In order to examine the effect of the pre-irradiation, the mobility and the lifetimes for both carriers were experimentally evaluated. The carrier mobility was acquired by measuring the traveling time of each carrier generated by a 5 MeV α -particle injected through one electrode side. Gamma-ray response pulses obtained from the pre-irradiated detector were collected with a fast digital oscilloscope (LeCroy 9384) and their pulse shapes were analyzed to evaluate the lifetime. The mobility was 616 cm²/V·s for the electron and 60.7 cm²/V·s for the hole. The change of the mobility due to the pre-irradiation was not observed. Table 5.3 summarizes the lifetimes for the

individual detector. The pre-irradiated detector indicates large decreasing of the electron lifetime. The lifetime ratio changes from 0.78 to 0.3 and this change provides the pre-irradiated detector with different response characteristic.

Table 5.3 The lifetimes of the CdTe detectors.

	τ_e (μs)	τ_h (μs)	Ratio (τ_e/τ_h)
Original	4.9	6.3	0.78
Pre-irradiated detector	1.9	6.3	0.30

The spectroscopic performance for lower-energy photons was examined by comparing ^{241}Am pulse height spectra measured with both the detectors. Each detector was subjected with radiation from the negative contact side. Thus the radiation interaction positions are limited around the negative side due to the lower energy of the incident photons, and then the generated electrons are major for pulse formation in this case. The RTD processing was not employed. As shown in Fig. 5.4, the position of the 59.5 keV peak moves toward lower channels for the spectrum measured with the pre-irradiated detector. This peak shift is due to the change of the response characteristic of the detector. However, the spectrum shape seems not to change significantly. Actually, the Full Width at Half Maximum (FWHM) of a 59.5 keV peak was approximately 4.0 keV for both the detectors. Although the peak position changes slightly, the pre-irradiation treatment seems not to change the energy resolution on the measurement of low-energy photons.

5. 4. 2 Spectroscopic Performance for High-energy Photons

The spectroscopic performance for high-energy photons was examined. Figure 5.5 presents ^{133}Ba spectra obtained from the original and the pre-irradiated CdTe detector. These measurements were performed without the RTD processing and each measurement time was set to be the same. The time constant of the pulse shaping was

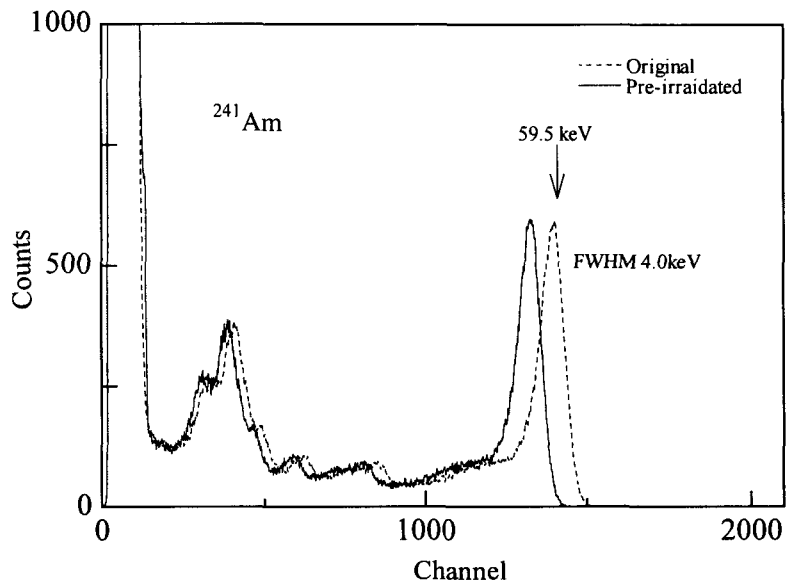


Fig. 5.4 ^{241}Am pulse height spectra measured with the CdTe detectors.

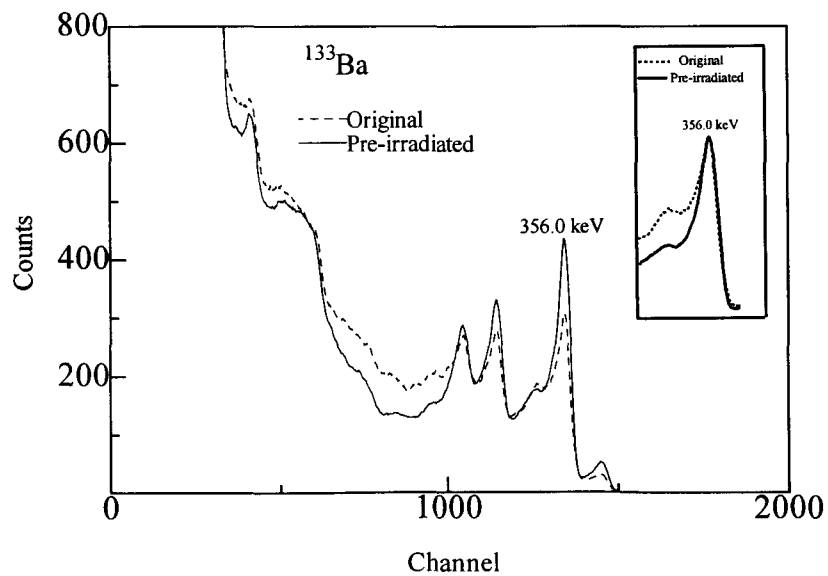


Fig. 5.5 Pulse height spectra of ^{133}Ba measured with the CdTe detectors. The peak shapes of the 356 keV peaks are compared in the window.

2 μ s. The spectrum of the pre-irradiated detector is shifted to higher channels (5 %) for detailed comparison. In this figure, the spectrum shape in the energy range around 300 keV is focused. Although four photopeaks can be identified in both spectra, the peak to valley ratio of the photopeak becomes relatively better for the spectrum by the pre-irradiated detector. The energy resolution was approximately 21 keV (FWHM) at 356 keV for the original and 15 keV for the pre-irradiated detector. Additionally, the counting ratio of the photopeak becomes larger than that for the original. This result indicates that the suppression of the amplitude fluctuation leads to the relative increase of the counting ratio at the peak position. The pre-irradiation effect can be clearly shown by comparing the shape of the photopeak as indicated in the window in Fig. 5.5. Each peak height was arranged to be equal by changing the measurement time. The peak tailing to lower channels is apparently observed for the original. This peak tailing is originated from the amplitude fluctuation, resulting in poor peak to valley ratio. From these results, it was found that the pre-irradiation treatment improved the response characteristic of the CdTe detector.

5. 4. 3 Performance with RTD Processing System

Figure 5.6 shows ^{133}Ba spectra acquired from the CdTe detectors. Three measurement conditions are compared; (a) the original without RTD, (b) the original with RTD and (c) the pre-irradiated detector with RTD. The rise time width for pulse collection was set to be 0.4-0.8 μ s when using the RTD processing. As shown in Figs. 5.6b and c, energy resolution is markedly improved by the RTD processing. Especially, the combination of the pre-irradiated detector and the RTD processing shows superior resolution among the three conditions. It is notable that the escape peak of the 356 keV peak can be identified in Fig. 5.6c.

Figure 5.7 shows the ^{137}Cs spectra taken by the RTD processing. The spectra with different rise time width were compared to examine the response characteristic of the pre-irradiated detector. For convenience, the peak height of the 662 keV peak is adjusted to be almost the same by changing the measurement time of each case. It is shown that the RTD processing provides better energy resolution for both the detectors. However, the peak tailing appears as shown in Fig. 5.7a when the rise time width

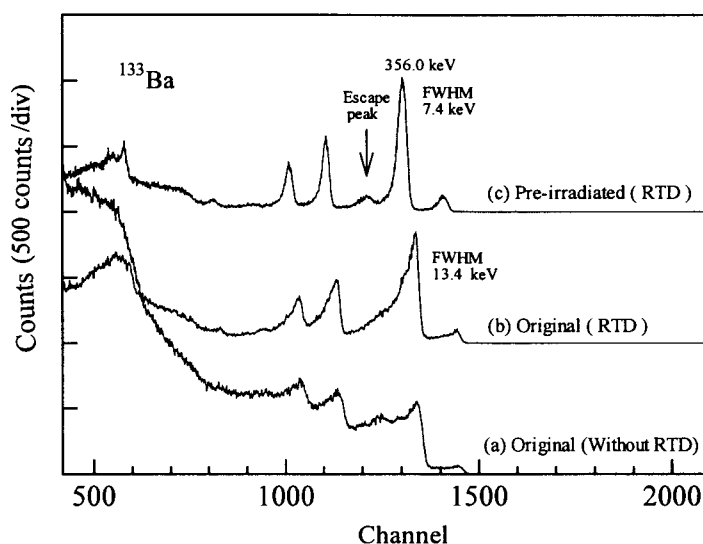


Fig. 5.6 Pulse height spectra of ^{133}Ba measured with the CdTe detectors; (a) original without RTD, (b) original with RTD and (c) the pre-irradiated detector with RTD.

increases. This result indicates that the energy resolution is still dependent on the amplitude fluctuation of the collected pulses. In contrast, the pre-irradiated detector provides good energy resolution in all rise time range as shown in Fig. 5.7b. Figure 5.8 presents the change of the energy resolution as a function of the rise time width. For the original, the FWHM of the 662 keV photopeak shows linear increase with increasing the rise time width. However the one for the pre-irradiated detector is located around 18 keV and its change is slight. This result can be explained by the fact that the pulse amplitude fluctuation in wide rise time range is suppressed by the pre-irradiation treatment.

The plateau response function contributes the improvement of the pulse collection efficiency. When using the RTD processing, narrow rise time width is employed to obtain higher resolving power, and therefore the collection efficiency markedly decreases. Hence the “effective” pulse which contributes spectrum formation decreases significantly and this leads to the poor collection efficiency of the detector. On the other hand, the energy resolution strongly depends on the rise time width for

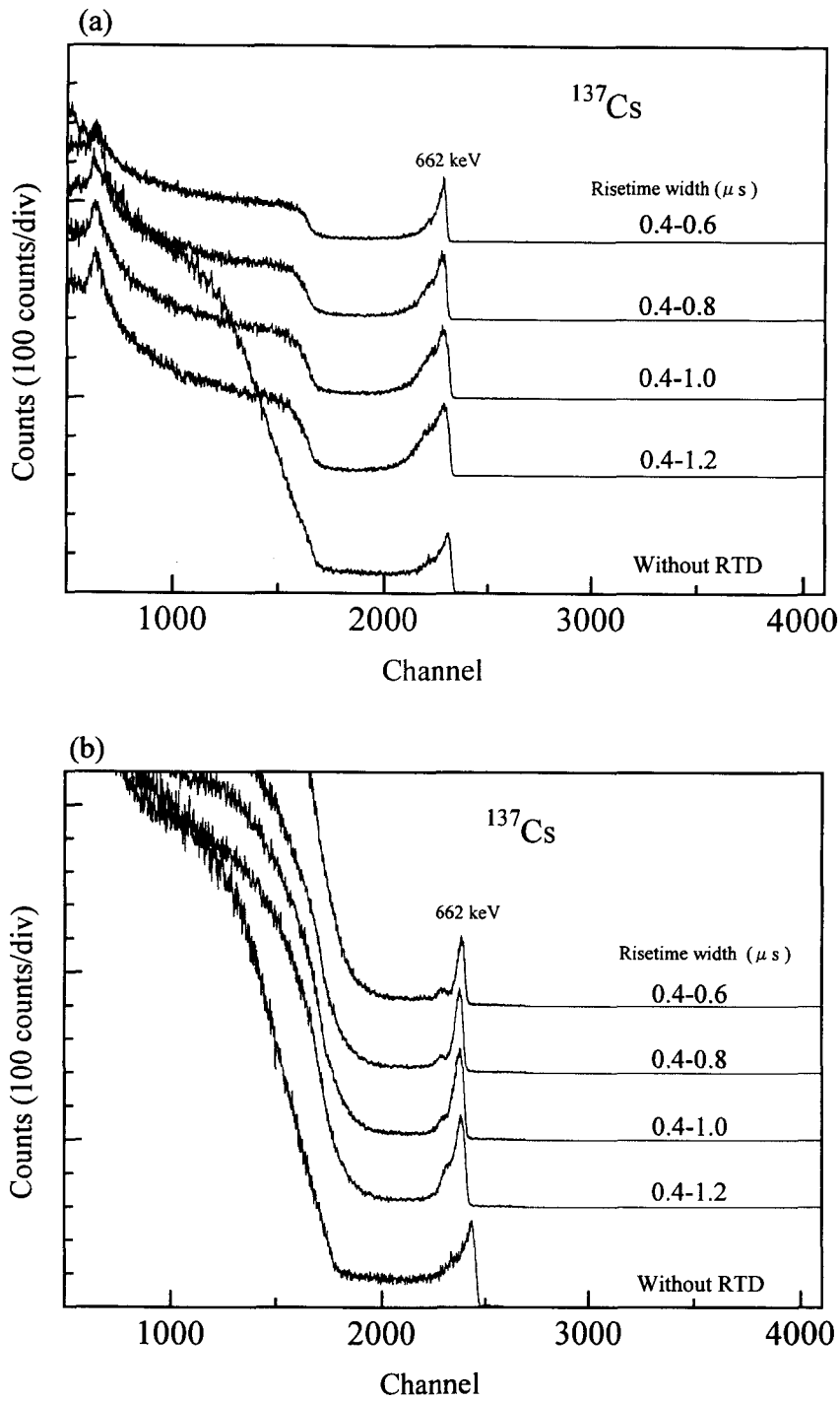


Fig. 5.7 Stacked plot of ^{137}Cs pulse height spectra measured with; (a) original, (b) pre-irradiated CdTe detector. The rise time width corresponds to the range of the pulse collection.

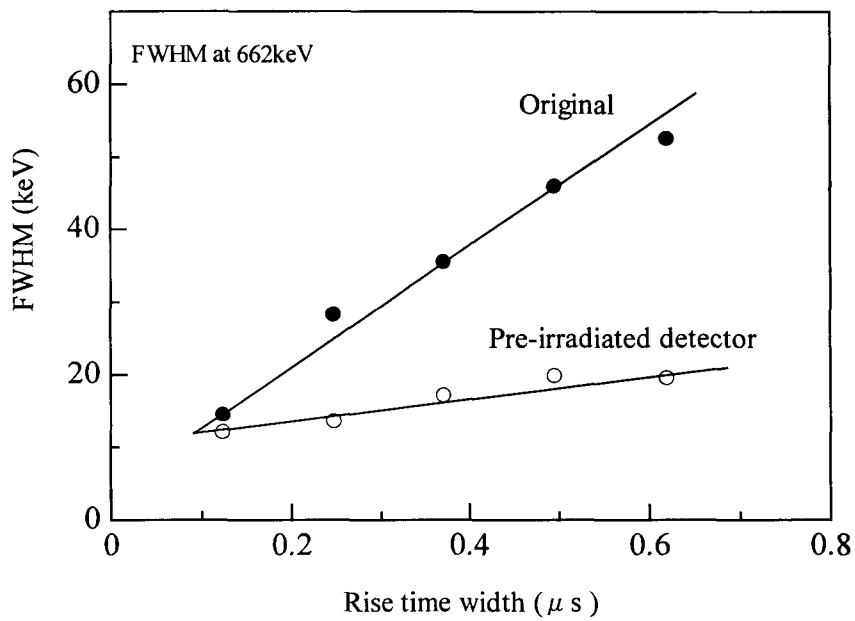


Fig. 5.8 Evolution of the FWHM as a function of the rise time width.

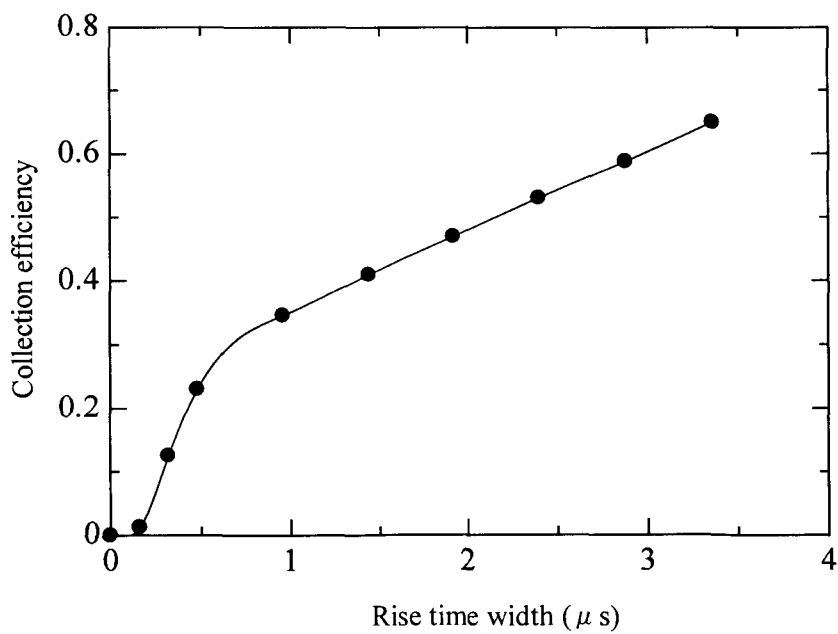


Fig. 5.9 The collection efficiency as a function of the rise time width. The efficiency is normalized by the one without using the RTD.

pulse collection. Figure 5.9 shows the experimentally obtained result of the collection efficiency changing with the rise time width. The efficiency is normalized by the one measured without RTD. The collection efficiency decreases gradually with decreasing the rise time width. From the data of Figs. 5.8 and 5.9, it can be found that the collection efficiency for each detector differs when the energy resolution is set to be the same level. For instance, the rise time width for pulse collection should be approximately 0.2 μs for the original and 0.7 μs for the pre-irradiated detector if the energy resolution of 20 keV is required. In this case the efficiency of the original detector becomes only 4.7 %, while the pre-irradiated one keeps approximately 31 %. Consequently the plateau response function of the pre-irradiated detector is effective to improve the collection efficiency on the RTD system.

5. 4. 4 Performance Stability

It is important to examine performance stability in time for the pre-irradiated CdTe detector. Especially, the persistency of the pre-irradiation effect should be required to maintain stable performance of the detector. For long use at room temperature, significant change of the performance has not been observed over a period of a few years in this study. Moreover, neither polarization ^{(8),(24)} nor the fluctuation of the noise level was observed. The performance stability of the pre-irradiated CdTe detector seems to be enough for use at room temperature.

5. 5 Conclusion

The treatment of fast neutron pre-irradiation was employed to improve the response characteristic of the CdTe detector. The response characteristic was changed by the pre-irradiation treatment to decrease the amplitude fluctuation in rise time. The peak tailing of the full energy peak was suppressed by this treatment. Additionally, the combination of the pre-irradiated detector and the RTD processing was found to provide further enhancement of the energy resolution on the measurement of high-energy photons. The effectiveness of the fast neutron pre-irradiation to the CdTe detector was demonstrated. In general, the transport properties of both carriers show simultaneous

change with the operating temperature and/or the applied bias^{(15),(19)}. Therefore it seems to be difficult to change the response characteristic as desired by such change of the operating condition. On the other hand, the treatment of fast neutron pre-irradiation allows us to change the characteristic flexibly because it affects only the motion of electrons. Also, fast neutron irradiation does not change chemical characteristics of the CdTe and it influences homogeneously to whole volume of the CdTe crystal. The pre-irradiation treatment directly changes the intrinsic response characteristic of the CdTe detector. Recently the performance of CdTe/CZT detectors has been improved by using several technological developments such as electrical signal processing^{(6),(18)}, arrangement of the electrode structure⁽²⁵⁾ and so on. However, these developments require additional electrical circuits or instruments for the spectroscopy. The important point is that the treatment of fast neutron pre-irradiation do not spoil the advantage of the CdTe detector such as usability and portability. In view of productivity, the pre-irradiation treatment seems to be somewhat less practical. However, our study proposed that positive control of the transport characteristic was one way to improve the detector performance. Further study of fast neutron irradiation effects will provide new applications for semiconductor-type radiation detectors.

References

1. H. Miyamaru, T. Iida, and A. Takahashi, *J. Nucl. Sci. and Tech.*, Vol. 36, No.1, (1999).
2. Squillante, M. R. and Entine, G.: *Nucl. Instrum. and Methods.*, A322, 569 (1992).
3. Sheiber, C. and Chambron, J.: *Nucl. Instrum. and Methods.*, A322, 604 (1992).
4. Eisen, Y.: *Nucl. Instrum. and Methods.*, A322, 596 (1992).
5. Baldazzi, G. et al.: *Nucl. Instrum. and Methods.*, A322, 644 (1992).
6. Schlesinger, T. E. and James, R. B.: "Semiconductors for Room Temperature Nuclear Detector Applications", Academic Press, Vol. 43, New York, (1995).
7. Eisen, Y. and Horovitz, Y.: *Nucl. Instrum. and Methods.*, A353, 60 (1994).
8. Mergui, S. et al.: *Nucl. Instrum. and Methods.*, A 322, 381 (1992).
9. Khusainov, A. Kh.: *Nucl. Instrum. and Methods.*, A 322, 335 (1992).
10. Ohmori, M. et al.: *Mat. Sci. and Eng.*, B16, 283 (1993).

11. Biglari, B. et al.: J. Appl. Phys., 65 (3), 1112 (1989).
12. Shoji, T. et al.: IEEE Trans., Nucl. Sci., Vol. 40, No.4, 405 (1993).
13. Caillot, M.: Nucl. Instrum. and Methods., 150, 39 (1978).
14. Verger, L. et al.: Nucl. Instrum. and Methods., A322, 35 (1992).
15. Taguchi, T. et al.: Nucl. Instrum. and Methods., 150, 43 (1978).
16. Miyamaru, H. et al.: J. Nucl. Sci. and Tech., Vol. 33, No 9, 744 (1996).
17. Miyamaru, H. et al.: J. Nucl. Sci. and Tech., Vol. 34, No 8, 755 (1997).
18. Richter, M. and Siffert, P.: Nucl. Instrum. and Methods., A 322, 529 (1992).
19. Siffert, P.: Nucl. Instrum. and Methods., 150, 1 (1978).
20. Zanio, K. R. et al.: J. Appl. Phys., Vol.39, No 6, 2818 (1968).
21. Manfredotti, C. et al.: Nucl. Instrum. and Methods., A 322, 331 (1992).
22. Scannavini, M. G. et al.: Nucl. Instrum. and Methods., A 353, 80 (1994).
23. Sumita, K. et al.: Nucl. Sci. Eng. 106, 249 (1990).
24. Siffert, P. et al.: IEEE trans., Nucl. Sci., Vol NS-23, No 1, 159 (1976).
25. Luke, P.N.: IEEE trans., Nucl. Sci., Vol 42, No 4, 207 (1995).

Chapter 6

Summary

In order to clarify the relationship between radiation effects and the performance change of the CdTe detector, the irradiation experiments with 14 MeV fast neutrons and deuterium ions were conducted in this study. The findings are summarized as follows.

1. Influence of fast neutron irradiation

The influence of fast neutron irradiation on the CdTe detector was clarified from this study for the first time. The electron lifetime significantly decreased for the detector irradiated with 14 MeV fast neutrons. In contrast, the transport property of holes showed almost unchanged. From the two-dimensional spectrum analysis, the electron trapping was found to occur for the irradiated detector. The experimental results of the isochronal annealing and the TSC analysis indicated that the characteristics of the deep electron-trapping center was similar to that of the Cd-related one. Radiation hardness of the CdTe detector against 14 MeV fast neutrons is summarized as: The detector keeps its spectroscopic performance in the fluence below 1×10^{10} n/cm² for conventional use. However, the performance is maintained until the fluence of 1×10^{11} n/cm² when the hole is employed as a major carrier for the radiation response.

2. Deuterium ion implantation effect

Deuterium ion implantation effect was investigated for the CdTe detector. When the concentration of D locates less than 1×10^{13} ions/cm² in the CdTe, the implanted D atoms cause the passivation of the intrinsic defects of CdTe. The electron mobility

showed approximately 5 % increase comparing with that for before implantation. However higher concentration decreased both the carrier mobilities.

3. Applicability of two-dimensional spectrum analysis for the examination of radiation effects

Two-dimensional spectrum analyses were undertaken as a new method to examine the irradiation effects of fast neutrons, gamma rays, and D ions. The change of carrier mobility and the effect of carrier trapping were directly observed from the change of the two-dimensional spectrum. The applicability of this method was clarified.

4. Effectiveness of fast neutron pre-irradiation for performance enhancement of CdTe detectors

The treatment of fast neutron irradiation was used to change the radiation response characteristic of the CdTe detector. The electron lifetime decreased by the irradiation effect, and due to this peak broadening of a photopeak was effectively suppressed. The FWHM of the 356keV photopeak changed from 21keV to 15keV and the effectiveness of the pre-irradiation treatment was attested. The combination of the pre-irradiated detector and the RTD processing showed further resolution enhancement. Application of the fast neutron irradiation to improve the performance of the CdTe detector was demonstrated in this study.

Appendix

Brief explanations for important keywords

Rise Time

Pulse rise time is defined as a time period in which the voltage amplitude of a radiation response pulse increases with time from 10 % of the maximum to 90 %.

Carrier Mobility (μ)

Carrier mobility is referred as a parameter which characterizes the motion of a charged carrier in a matter. The relation between the velocity (v) of the carrier and the carrier mobility (μ) is given as

$$v = \mu \cdot E,$$

where E is the amplitude of the applied electric field. The carrier mobility is basically determined from the nature of the material as indicated in Table 1. However it also depends on the temperature⁽¹²⁾ and the concentration of intrinsic/extrinsic defects. Generally, the carrier mobility becomes higher as the temperature decreases, and then low temperature operation of the CdTe detector leads to the performance enhancement. Higher mobility is advantageous to the performance of semiconductor-type radiation detectors.

Lifetime (τ)

When the charged carriers are generated by radiation, they require the specific time to traverse the whole volume of the detector; this time period is named as "Transit time". The transit time (T_o) is approximately given by

$$T_o = \frac{d^2}{\mu \cdot V},$$

where V is the applied voltage and d is the distance between two electrodes. During the drift of the carriers, some of them are trapped and/or detrapped by the defects locating in the volume. A lifetime (τ), corresponding with "mean free time", is defined as the mean time in which carriers are free from the state of the trapping. When the lifetime becomes shorter, the probability of the carrier trapping increases. Therefore the carrier collection efficiency of the detector is strongly dependent on this parameter. For the radiation response, the change of voltage amplitude in time is briefly expressed as

$$V(t) = \frac{Q_o}{C} \exp\left(-\frac{t}{\tau}\right),$$

where Q_o is the total charge generated by radiation and C is the device capacitance.

Acknowledgements

The author gratefully acknowledges Prof. Akito Takahashi who supported this study and has advised him the direction of the thesis. The author wishes to express his sincere thanks to Prof. Toshiyuki Iida for helpful suggestions and encouragement. The author appreciates Prof. Toshikazu Takeda for the advises of this thesis. The author is indebted to Prof. Motoji Ikeya, Prof. Tetsuo Tanabe and Prof. Shinsuke Yamanaka for constant encouragement. The author thanks to Mr. Keiji Fujii for supporting the present work. The author also thanks to Lecturer Isao Murata and Research associate Shigeo Yoshida for their kind helps and to Messrs. Hisashi Sugimoto and Jun Datemichi for the operation of the accelerator. The author is grateful to the following persons.

To Mr. Kentaro Ochiai for helpful discussions.

To Messrs. Osamu Takahashi, and Jun Asahara for supporting the experiments. Moreover, the author thanks all the members of the OKTAVIAN facility. Special thanks to Yasuko and Aki Miyamaru for their hearty encouragement.

List of Publications

Publications related to the thesis

1. H. Miyamaru, T. Iida and A. Takahashi, : “Improvement of Radiation Response Characteristic on CdTe Detectors using Fast Neutron Irradiation” , J. Nucl. Sci. and Tech., Vol. 36, No.1, (1999).
2. H. Miyamaru, K. Fujii, T. Iida and A. Takahashi, : “Effect of Deuterium Ion Implantation on CdTe Radiation Detectors” , J. Nucl. Sci. and Tech., Vol. 35, No.9, 679 (1998).
3. H. Miyamaru, K. Fujii, T. Iida and A. Takahashi, : “Effect of Fast Neutron Irradiation on CdTe Radiation Detectors”, J. Nucl. Sci. and Tech., Vol. 34, No.8, 755 (1997).
4. H. Miyamaru, K. Fujii, T. Iida and A. Takahashi, : “Influence of Fast Neutron Irradiation on Signal Response of CdTe Radiation Detectors”, J. Nucl. Sci. and Tech., Vol. 33, No.9, 744 (1996).
5. H. Miyamaru, K. Fujii, T. Iida and A. Takahashi, : “The influence of Neutron Irradiation on CdTe Radiation Detectors”, *Ionizing radiation*, Vol.22, No.3, 43 (1996).

Other publications

1. H. Miyamaru, T. Tanabe, T. Iida and A. Takahashi, : “An ESR Study of Heavily Ion-irradiated SiO₂ Glass”, Nucl. Instr. Meth. B, Vol. 116, 393 (1996).
2. H. Miyamaru, T. Tanabe T. Iida and A. Takahashi, : “The Role of Implanted Deuterium on Defect Formation in SiO₂ Glass”, Proc. Int. Symp. on Material Chemistry in Nuclear Environment., 741 (1996).
3. H. Miyamaru, Y. Chimi, T. Inokuchi and A. Takahashi, : “Search for Nuclear Products of Cold Fusion”, Trans. of Fusion Technol., Vol.26, No.4, 2, 151 (1994).
4. H. Miyamaru and A. Takahashi, : “Periodically Current-controlled Electrolysis of

- D₂O/Pd System for Excess Heat Production”, “Frontiers of Cold Fusion”, Univ. Academy Press, Inc., 393 (1993).
5. H. Miyamaru and M. Ikeya, : “One-dimensional Scanning ESR Microscope Using Microwire-array”, Appl. Radiat. Isot., 44, 397 (1993).
 6. A. Takahashi, K. Maruta, K. Ochiai, H. Miyamaru, and T. Iida, : “Anomalous Enhancement of Three-body Deuteron Fusion in Titanium-deuteride Under the Stimulation by Deuteron Beam”, Fusion Technology, Vol. 34, 256 (1998).
 7. K. Ochiai, K. Maruta, H. Miyamaru, and A. Takahashi, : “Measurements of High-energetic Particles from Titanium Sheet Implanted with Deuteron Beam”, Proc. ICCF7, 274 (1997).
 8. M. Fujiwara, T. Tanabe, H. Miyamaru, and K. Miyazaki, : “Ion-induced Luminescence of Silica Glasses”, Nucl. Instr. Meth. B, Vol. 116, 536 (1996).
 9. K. Ochiai, T. Iida, N. Beppu, K. Maruta, H. Miyamaru, and A. Takahashi, : “Deuteron Fusion Experiments in Metal Foil Implanted with Deuteron Beams”, Proc. ICCF6, 377 (1996).
 10. A. Takahashi, T. Iida, H. Miyamaru and M. Fukuhara, : “Multibody Fusion Model to Explain Experimental Results”, Fusion Tech., Vol. 27, 71 (1995).
 11. T. Iida, M. Fukuhara, Sunaruno, H. Miyamaru and A. Takahashi, : “Deuteron Fusion Experiment with Ti and Pd Foils Implanted with Deuteron Beams II”, Trans. Fusion Tech., Vol.26, No.4, 2, 380 (1994).
 12. M. Ikeya, K. Megro, H. Miyamaru and H. Ishii, : “Educational Experiments on ESR Imaging with a Portable ESR Spectrometer”, Appl. Magn. Res. 2, 663 (1991).
 13. M. Ikeya and H. Miyamaru, : “Chemical Heat Production of Pd Electrode Electrolytically Charged with Deuterium and Hydrogen”, Chem. Exp. Vol. 4, No. 9, 563 (1989).